Science with VLBI absolute astrometry

Leonid Petrov *NASA GSFC*

Why do we do VLBI surveys?

"And what do you do with them?"

"I administer them," replied the businessman. *"I count them and recount them. It is difficult. But I am a man who is naturally interested in matters of consequence."*

The little prince was still not satisfied.

"I put them in the bank."

"Whatever does that mean?"

"That means that I write the number of my stars on a little paper. And then I put this paper in a drawer and lock it with a key."

"And that is all?"

"That is enough," said the businessman.

"It is entertaining," thought the little prince. *"It is rather poetic. But it is of no great consequence."*

Why surveys are important?

- Surveys are **the foundation** of astrometry. They supply the grid of phase calibrators.

  The availability of this grid make possible differential astrometry: measurements of **parallaxes, proper motions** of interesting sources.

- Surveys **target a large sample** of sources.

  They make possible to study **a population** of sources;

- Analysis of survey observations require development of theoretical and empirical **geophysical models**.

  They stimulate **geophysical applications**
  of radioastronomy.

- Sifting through results of surveys, we can find **rare** and **the most interesting objects**.

I. State of fundamental radio astrometry on 2019.09.09:

sources detected: 16466 # sources observed: 29446

percentiles of accuracy:

20%	< 0.23	mas
26.7%	< 0.30	mas
50% (median)	< 0.84	mas
80%	< 2.3	mas
90%	< 4.9	mas
95.1%	< 10	mas

Flux density @ X-band: [0.003, 22] Jy, median: 61 mJy

Observed band:

22 GHz	7%
8 GHz	92%
5 GHz	62%
2 GHz	35%
Dual-band:	77%

Number of observing sessions

1	55%
1–2	68%
1–5	91%
10+	5%
100+	2%

Radio Fundamental Catalogue

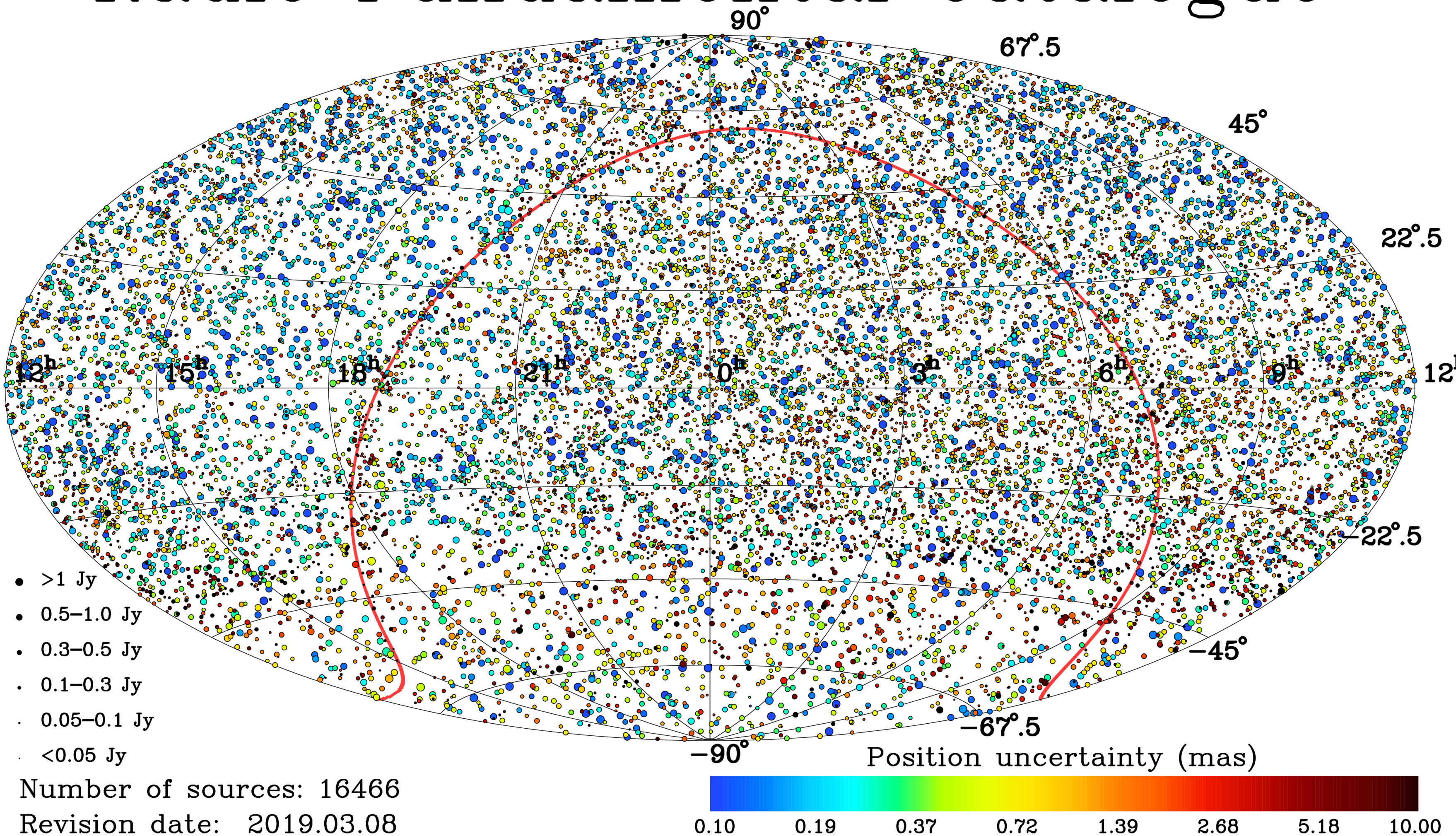

Number of sources: 16466

Revision date: 2019.03.08

Completeness of the RFC

$\log N$ versus $\log S$ diagram. $S_{\rm corr}$ @ 8 GHz at baselines 200–1000 km

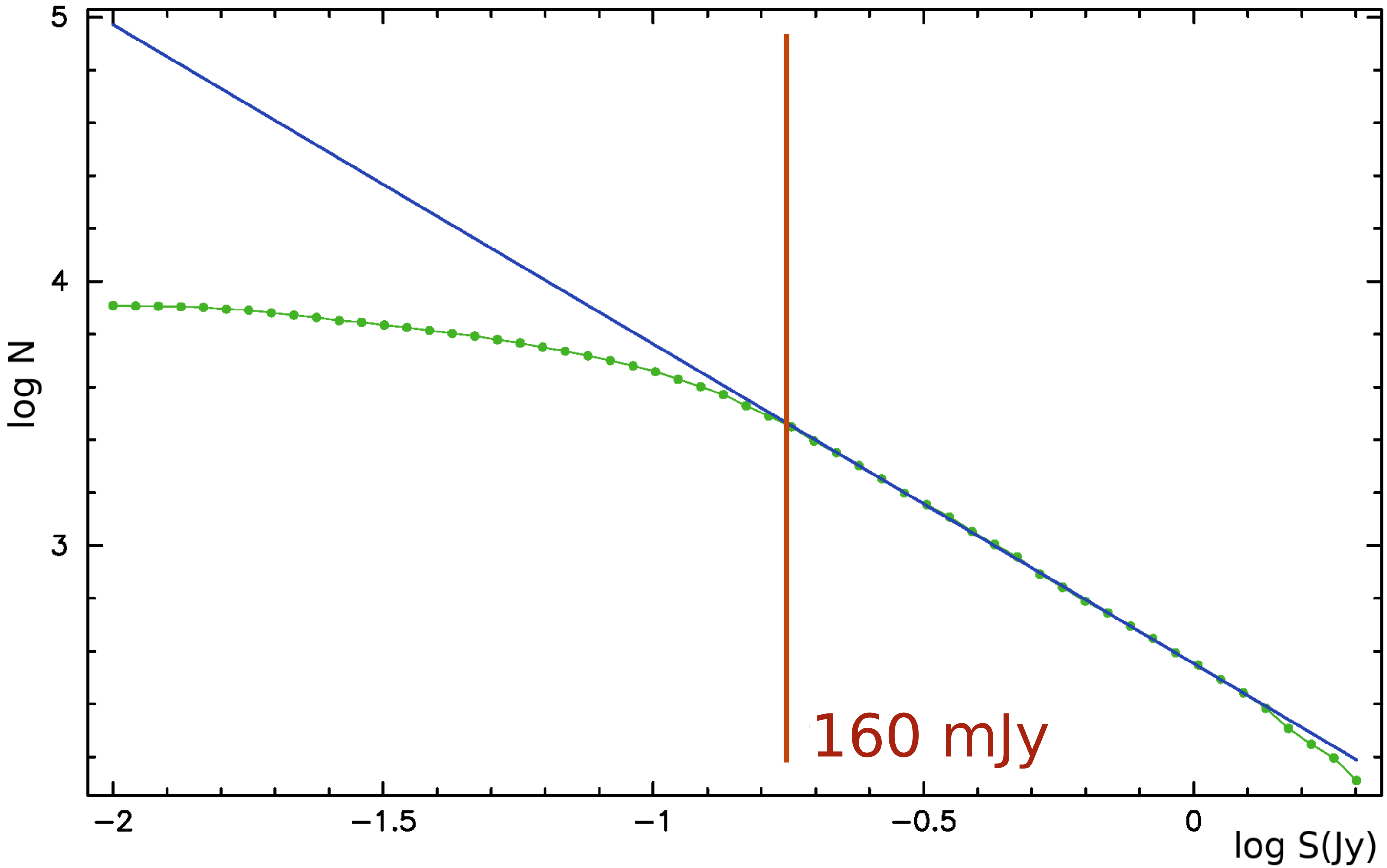

170 mJy	100%
160 mJy	98%
150 mJy	95%
100 mJy	82%
50 mJy	55%
10 mJy	14%

Source sky distribution (complete subsample of 3500 objects)

RFC (F(X) > 160 mJy)

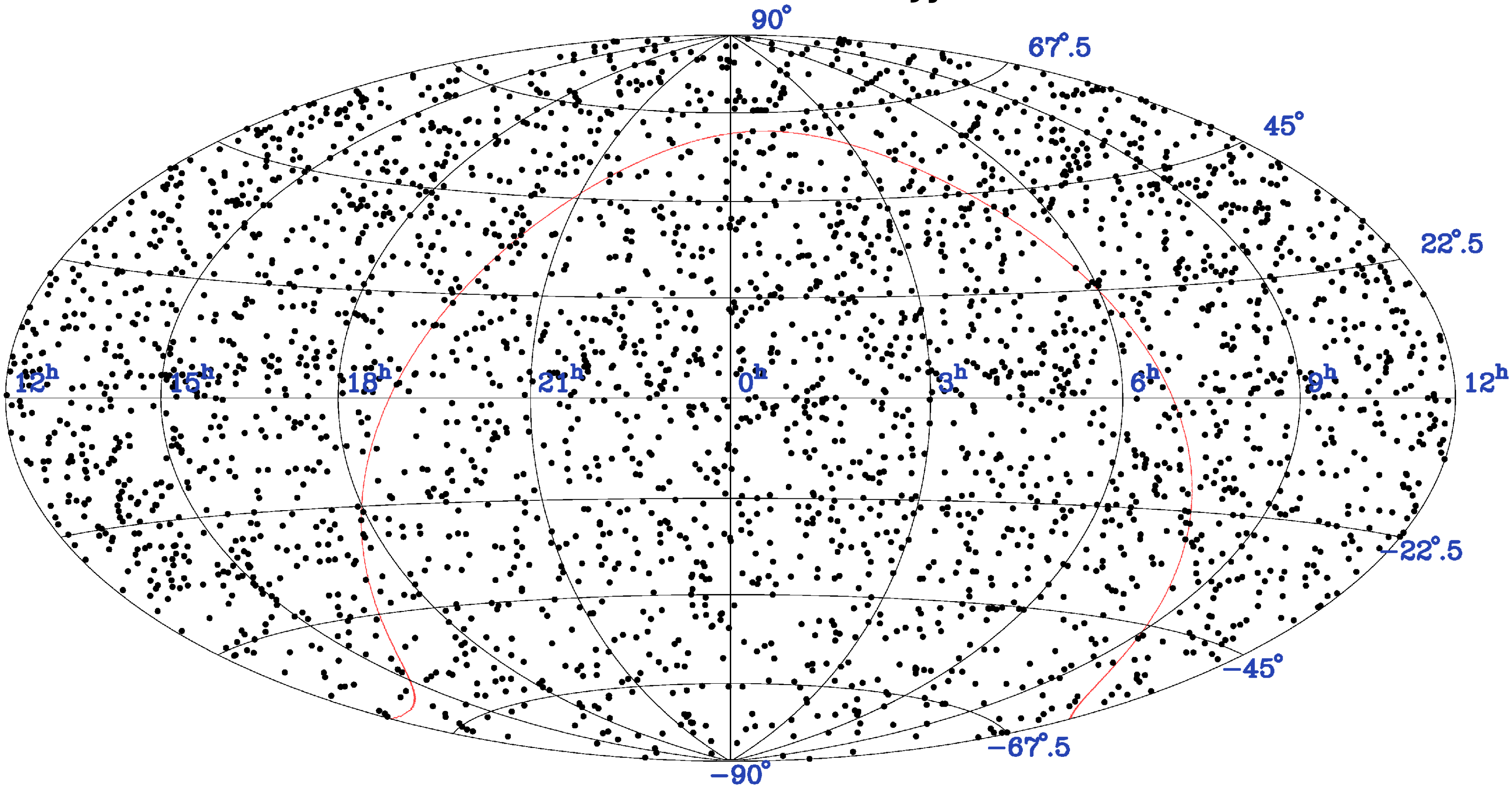

Comparison with Pan-STARRS catalogue

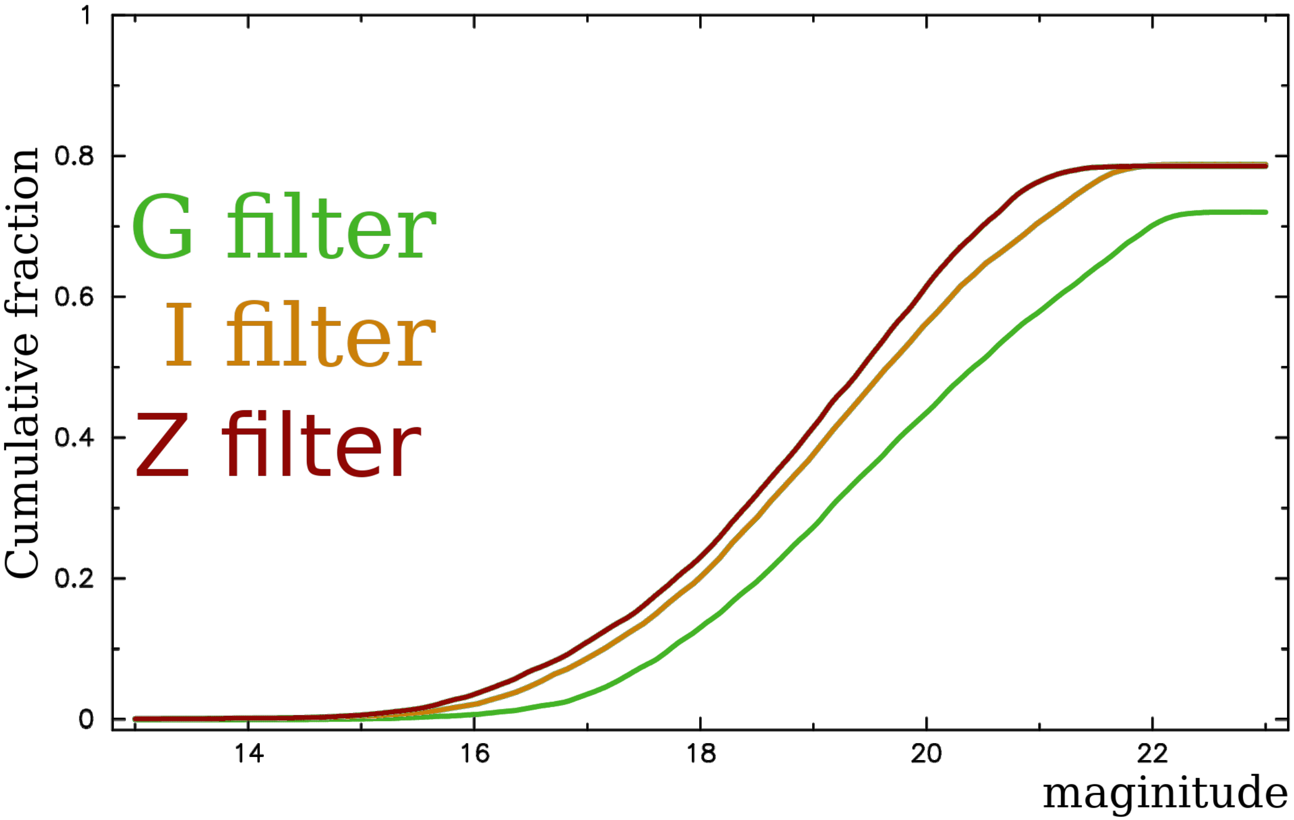

11391 RFC/PS matches

Flt	share	compl mag
g	72%	22.0
r	76%	21.8
i	79%	21.6
z	78%	21.0
y	74%	21.0

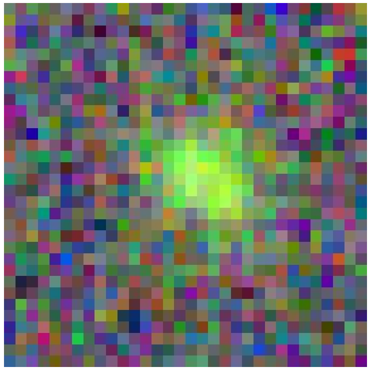

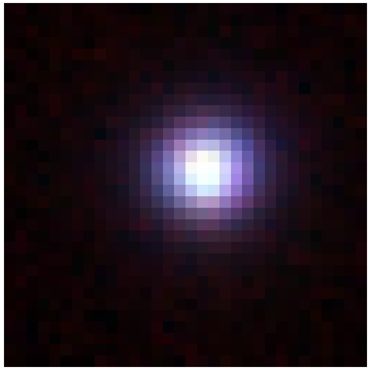

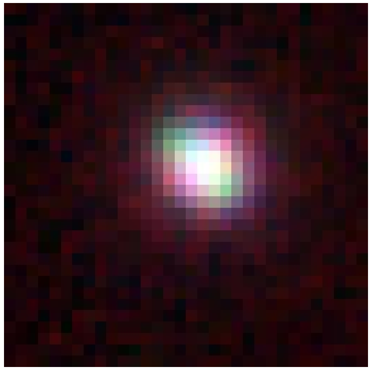

Number of matches

γ-ray	Fermi:	16%
X-ray	Chandra	5%
UV	Galex	34%
optic	Gaia:	60%
optic	PanSTARRS:	80%
infra-red	WISE:	74%

Observed objects

16452 Active galaxy nuclea

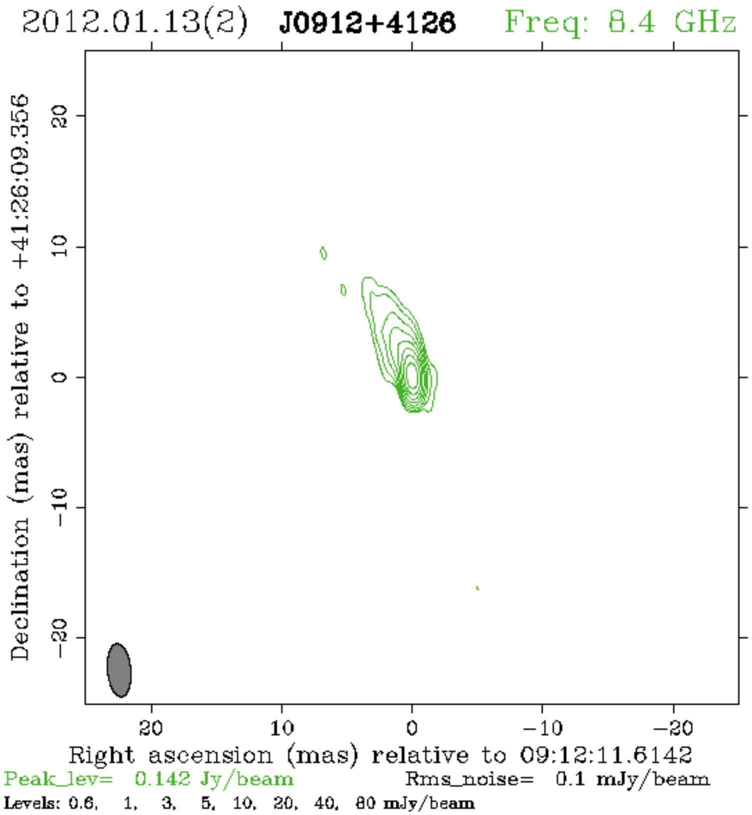

14 radio stars

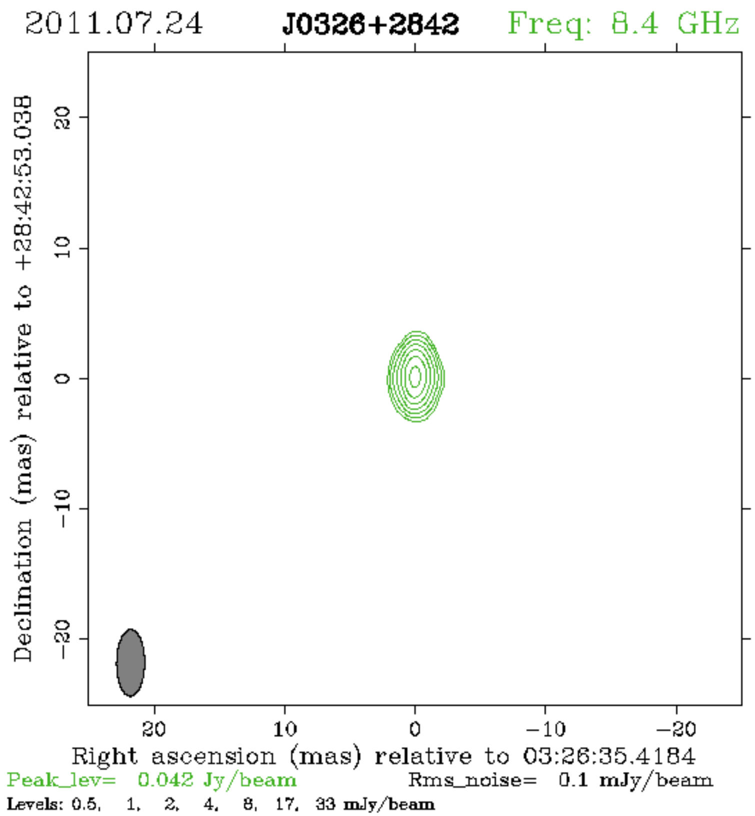

Observing campaigns

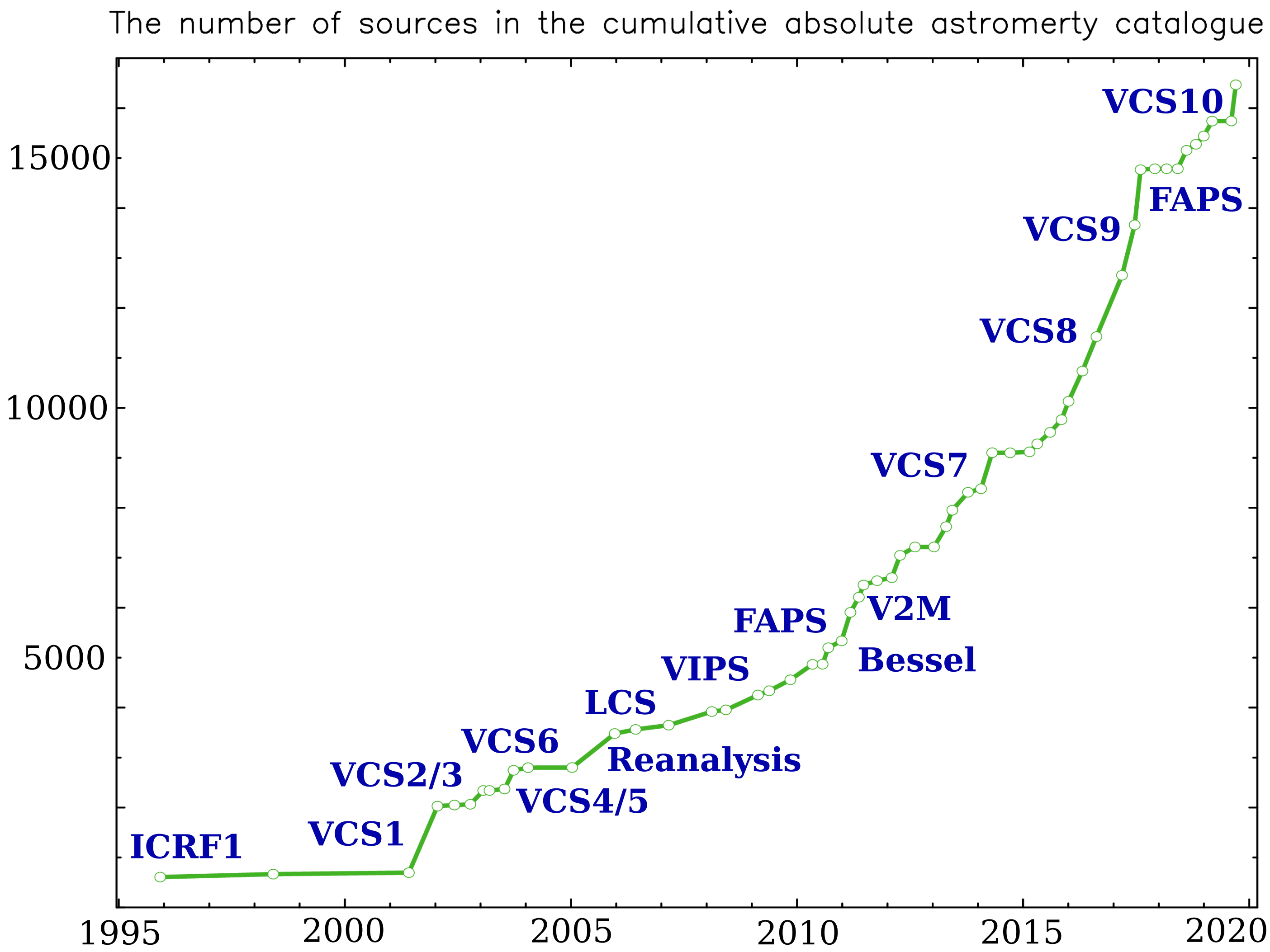

39 dedicated observing campaigns; 730 segments; 1.26 year observing time.
10 Pb raw data, 66 Tb visibility data.

Participating VLBI networks

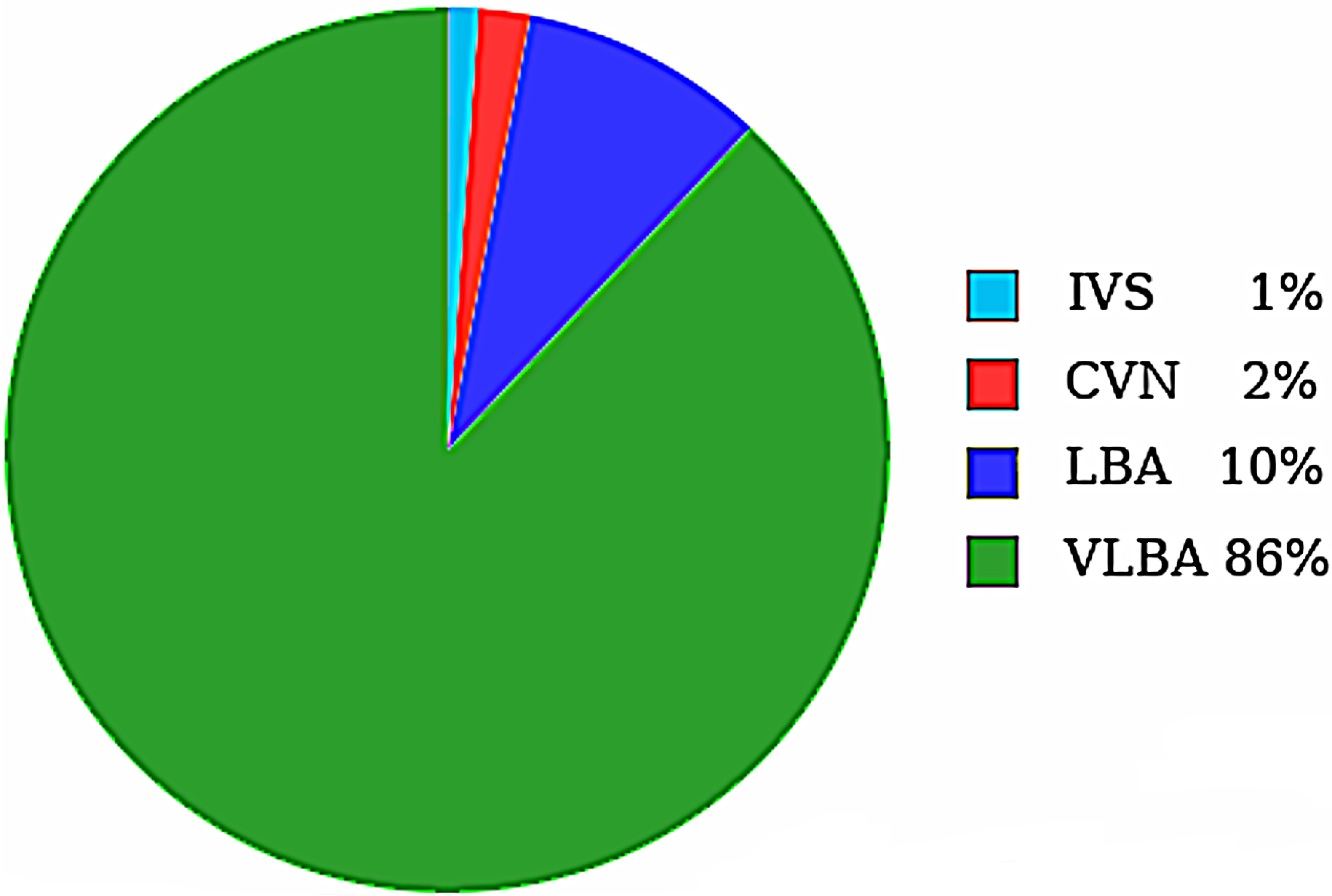

Technology of VLBI surveys

Source selection:

- Selection of a (wide) pool of candidates;
- Computing the probability of detection of each source;
- Maximization of the target function.
- Scheduling

A pool of candidates

- Surveys from connected interferometers (VLA, ATCA)
- Single dish observations (GB6)

Preference: high frequencies, high resolutions

Prediction of correlated flux density

Compactness $= F_{comp}/F_{tot}$

1. Spectrum:

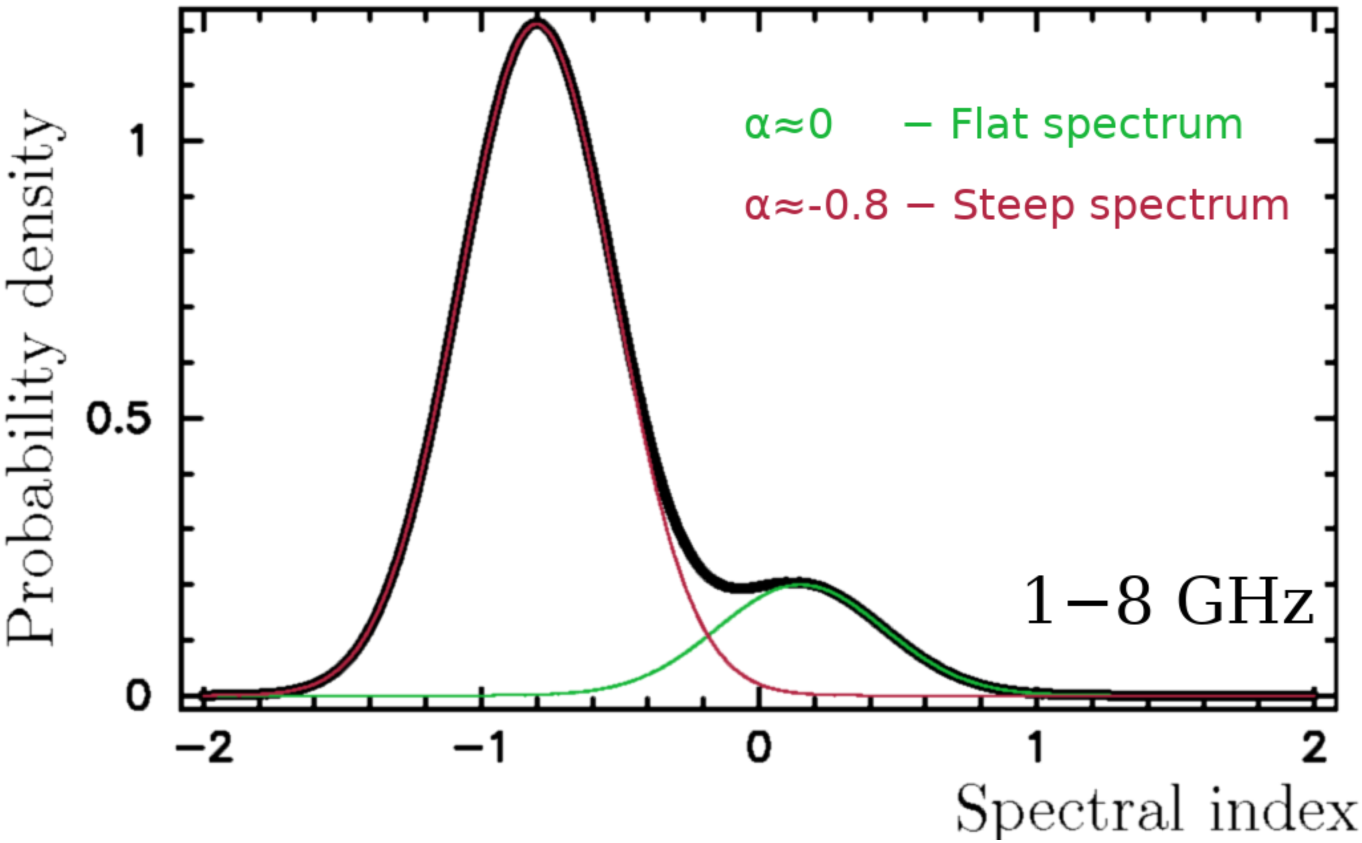

Sources with flat spectrum *in general* are more compact

2. Wise selection: WISE color-color diagram

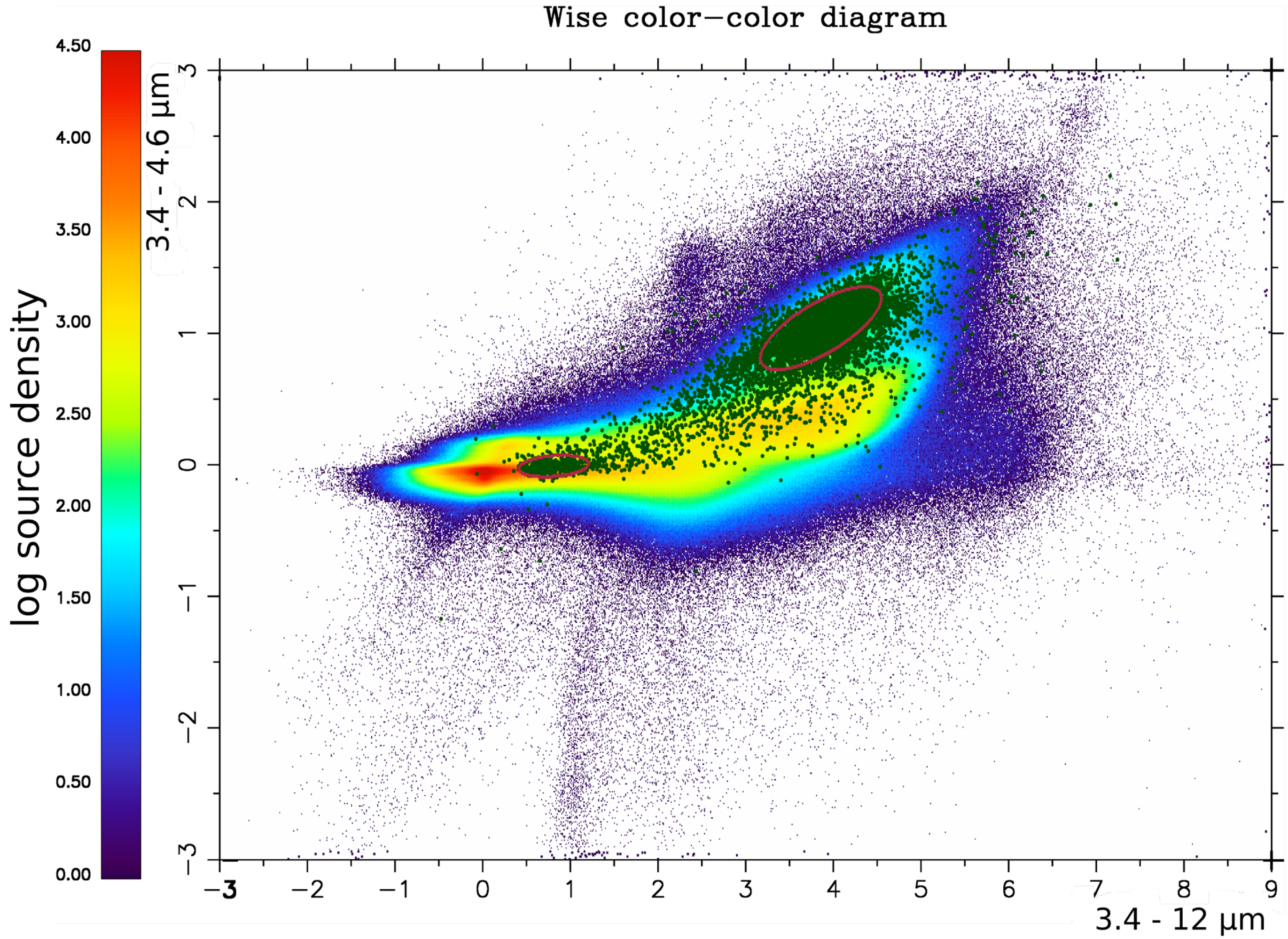

3. Frequency of observation:
   Sources detected at high frequencies are more compact

4. High energy counterpart:
   γ-ray sources are more compact

5. Galactic latitude:
   Sources at low galactic latitudes are less compact

6. Blind:
   disable filters

Survey optimization:

1. Formulate the target function, for example:
   - to maximize the total number of detected sources
   - to fill areas with low source density;
   - to reach completeness on correlated flux density
2. To find such a subset of candidate sources that maximize the target function.

Output: a source list and associated integration times.

Scheduling absolute astrometry surveys:

- determine the pool of candidate sources
- find a sequence of scans that minimizes slewing time and satisfy antenna constraints
- each source is observed in 1 to 8 scans depending on the schedule goal. The schedule goal sets the minimum time interval between scans.
- Insert every 1–2.5 hours calibrator sources. The purpose of calibrators:
  - to be able to solve for atmosphere path delay in zenith direction
  - to serve as amplitude calibrators for complex bandpass evaluation
  - to tie the positions with the core of frequently observed sources (absolutization).

  NB: The source list always **must** have an overlap.

Overheads for calibrator observations are 7–18% of on-source time.

VLBI surveys

- Increase the all-sky density of calibrators (VCS1–9,LCS)
- Observe special sources (f.e. γ-ray objects)
- Observe special zones (ecliptic, galactic plane, polar cap)
- High frequency follow-up (KQ,UD001)
- Reach completeness (VCS9,VCS10)

Nowadays, on average, 1 hour of observing time yields 13 newly detected sources.

Evolution of VLBI surveys

Originally (1990s) known bright flat-spectrum sources were observed.

Then we

- identified more flat spectrum sources
- selected the areas with low calibrator densities
- extended the field of view to the entire beam
- used 4.3/7.6 GHz instead of 2.3/8.6 GHz
- used automatic scheduling
- discarded selection based on spectral index

Why a wide field of view is needed?

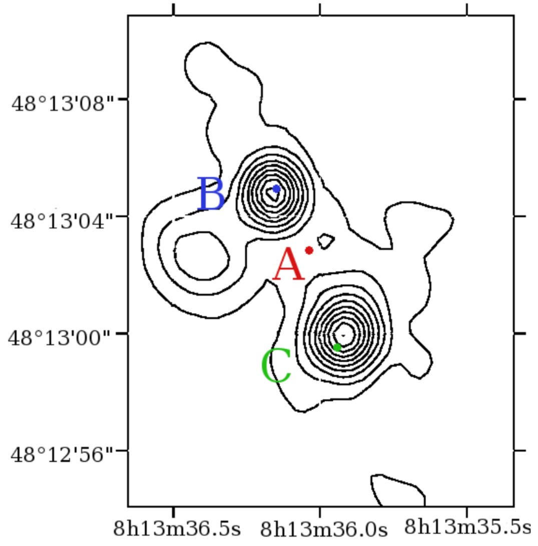

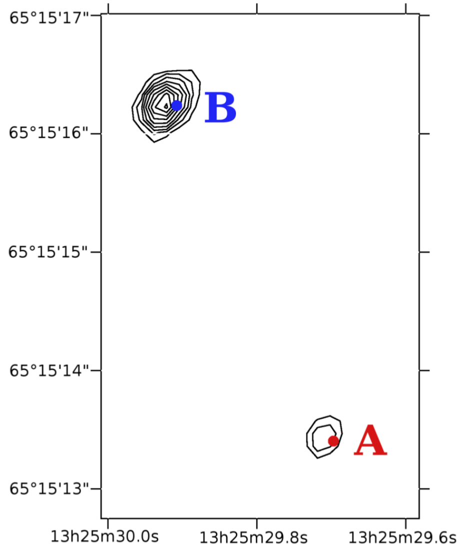

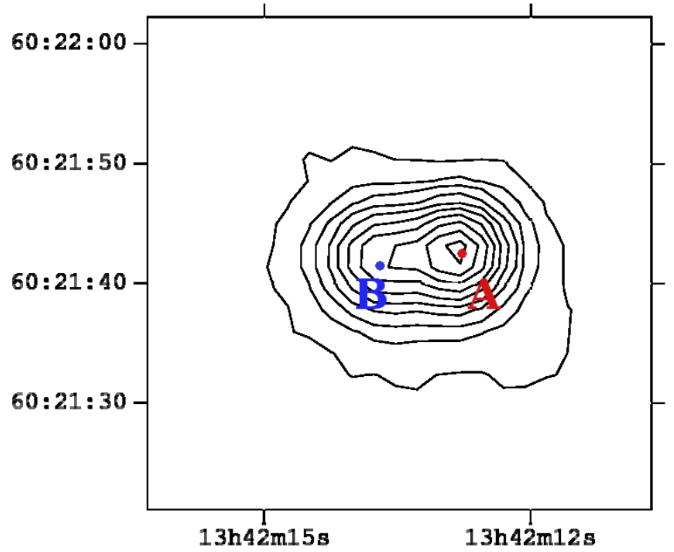

Where is the compact detail? **Look at the red point**

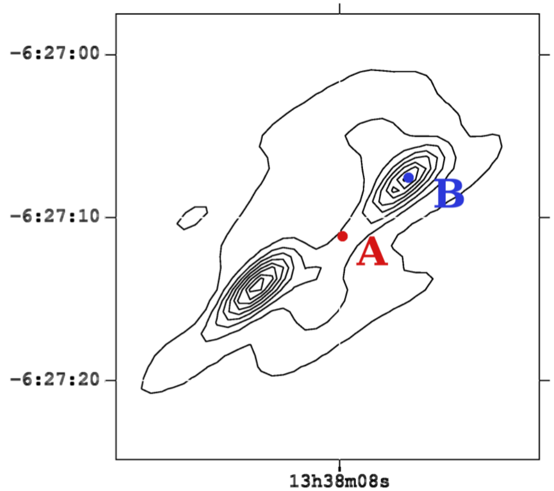

Flip-flopper sources

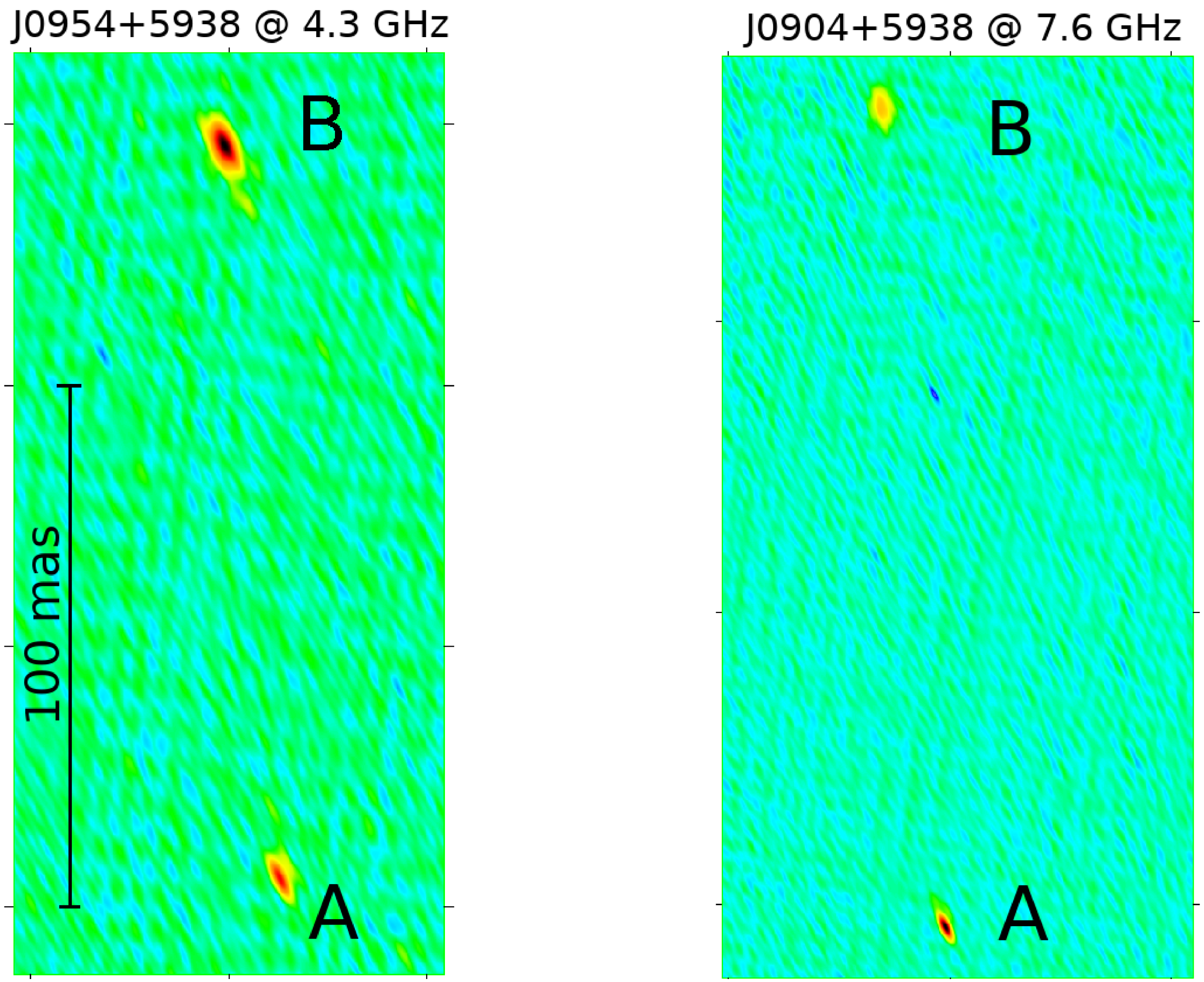

Comp	Brightness Jy/beam		Flux density Jy		
	4.3 GHz	7.6 GHz	4.3 GHz	7.6 GHz	
A	8.9	14.6	10.7	30.6	core
B	24.3	4.5	26.9	19.2	jet component

Snapshot images from VCS7–VCS8:

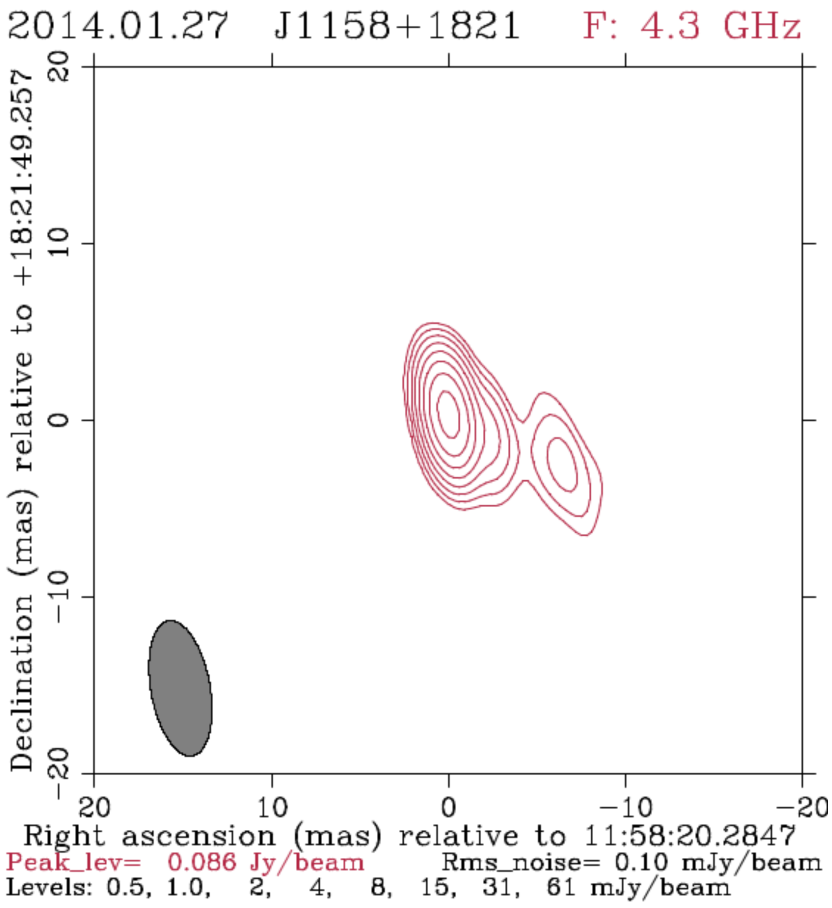

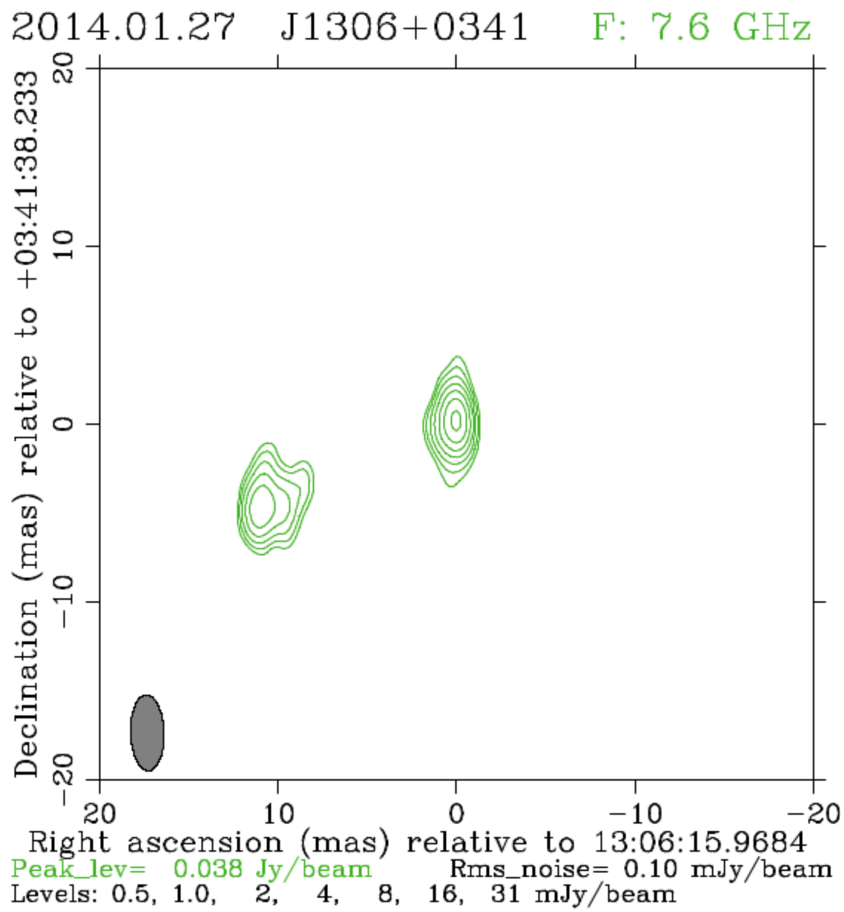

NB: Integration time is only 60 s!

Peculiar sources from VCS7–VCS8:

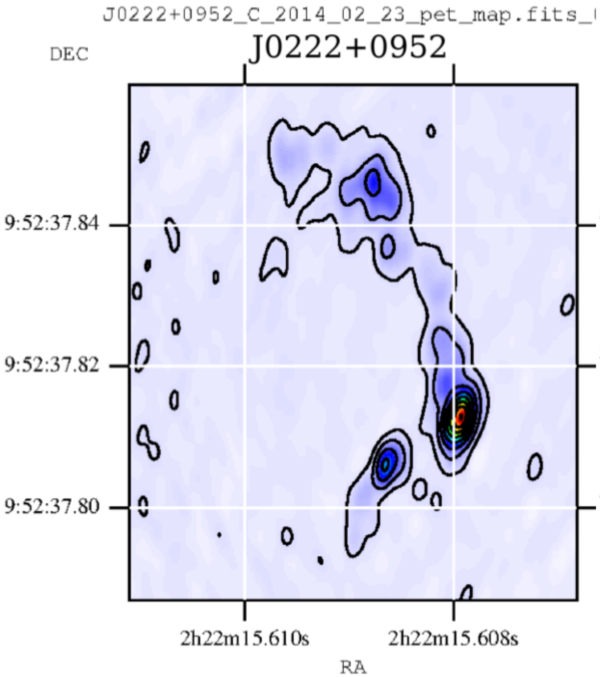

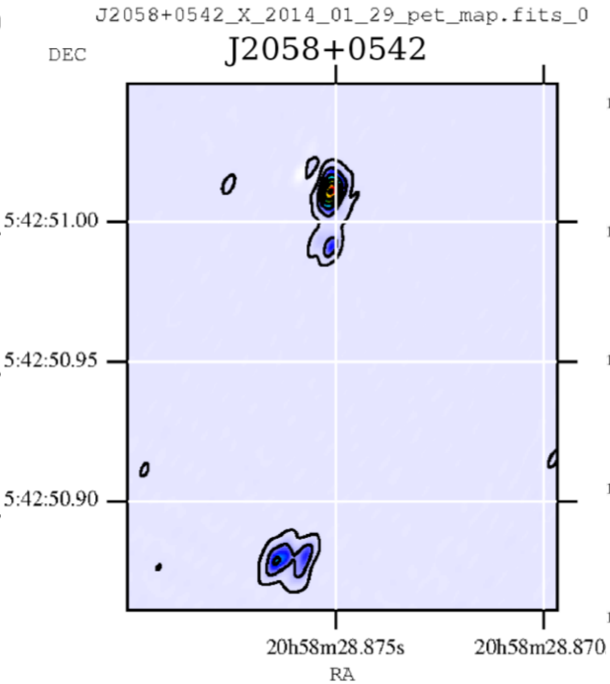

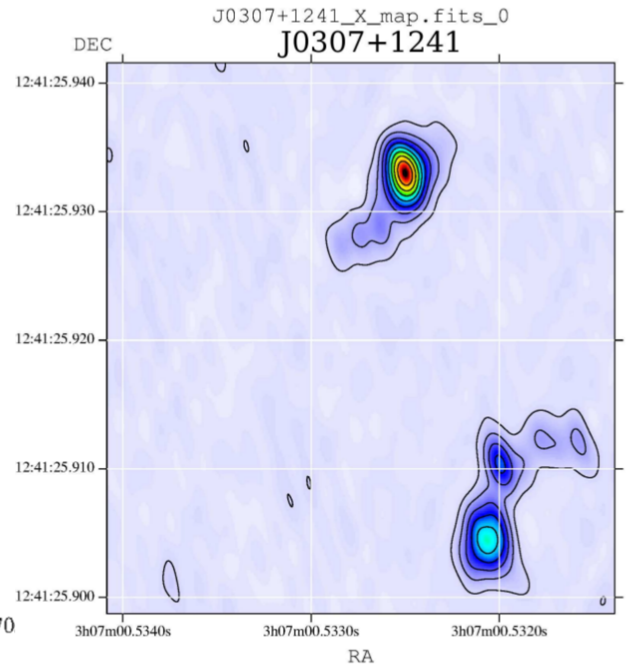

Spectral index distribution

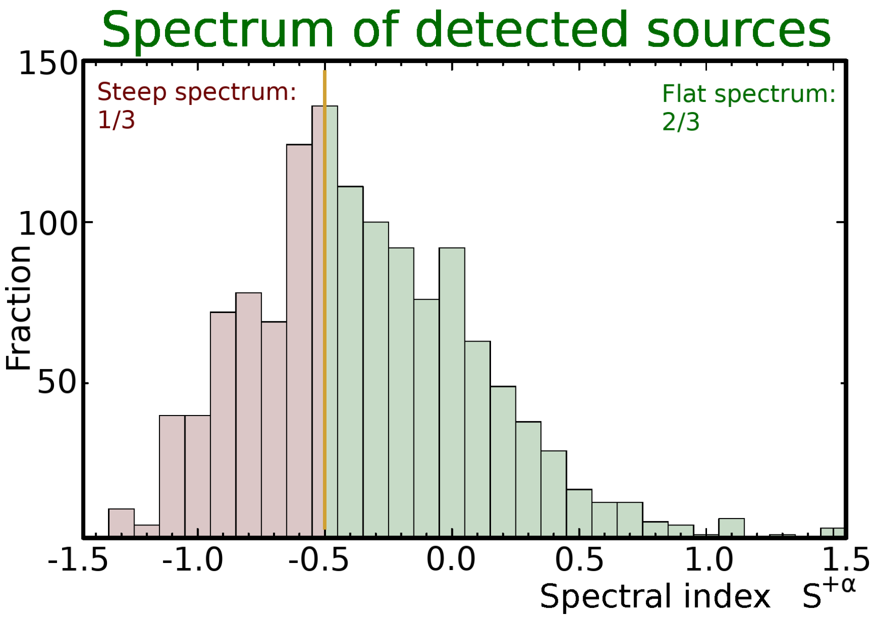

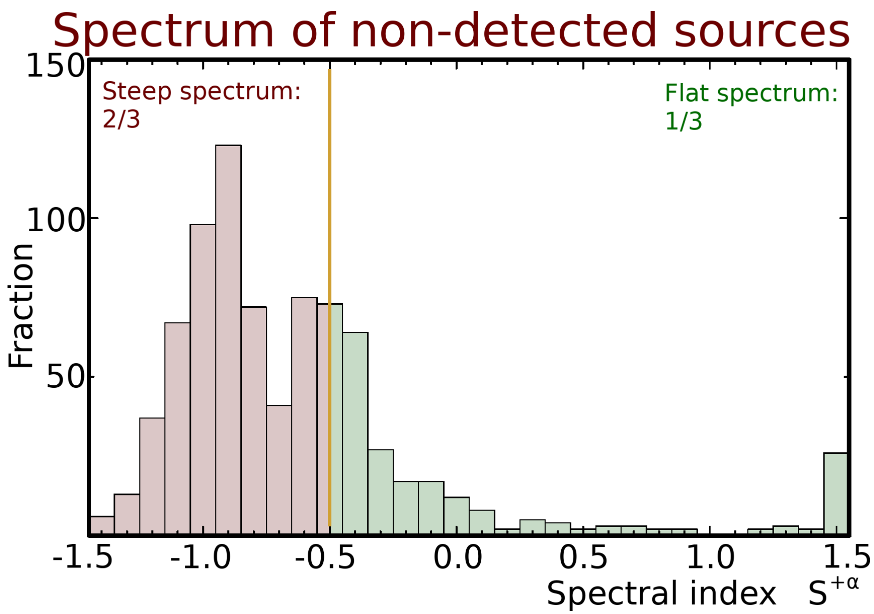

A rule of 1/3:

- 1/3 of detected sources have steep spectrum
- 1/3 of flat spectrum sources are not detected

Is the source distribution isotropic?

There are 13 pairs visually double radio sources with distances less than $1'$:

Dist			F_{corr}(8.6GHz)		Comment
$1.3''$	J1308+6544	J1306+665A	68	56	
$1.9''$	J2157+662A	J2157+662B	41	11	Double galaxy
$16.2''$	J0257+0601	J0257+060A	32	23	Double galaxy
$25.6''$	**J0635-262A**	**J0635-262B**	**172**	**142**	**different z**
$28.0''$	J2309-3632	J2309-363A	19	17	
$28.1''$	J1559+255A	J1559+2556	17	20	Double galaxy
$33.5''$	**J1041+523A**	**J1041+523B**	**495**	**62**	**different z**
$39.9''$	J1010-0200	J1010-020A	391	28	
$46.8''$	J1919+7433	J1919+7434	27	20	
$47.2''$	J0413-1619	J0413-1618	12	18	
$52.3''$	J1152+2312	J1152+2313	98	86	
$59.1''$	J1522+7645	J1523+7645	61	21	
$59.4''$	J1715+2146	J1715+2145	31	8	different spectra

Assuming isotropic sources distribution, the probability to find two pairs at $30''$ separations, J0635-262A/J0635-262B and J1041+523A/J1041+523B is only 0.0007.

VLBA image of J2157+6626:

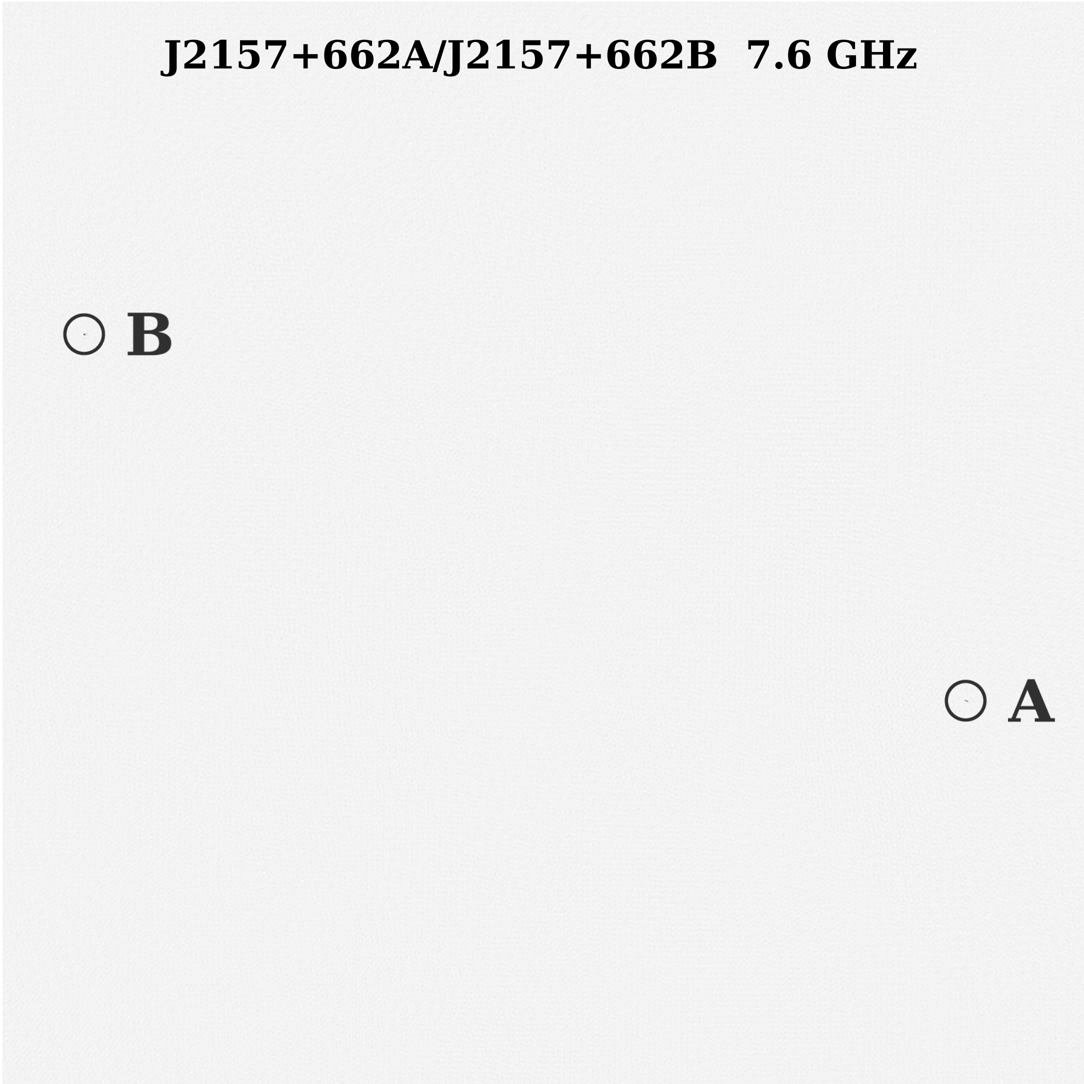

Distance A/B: 1".8894 (2.1 kpc)

VLBA images of J2157+6626:

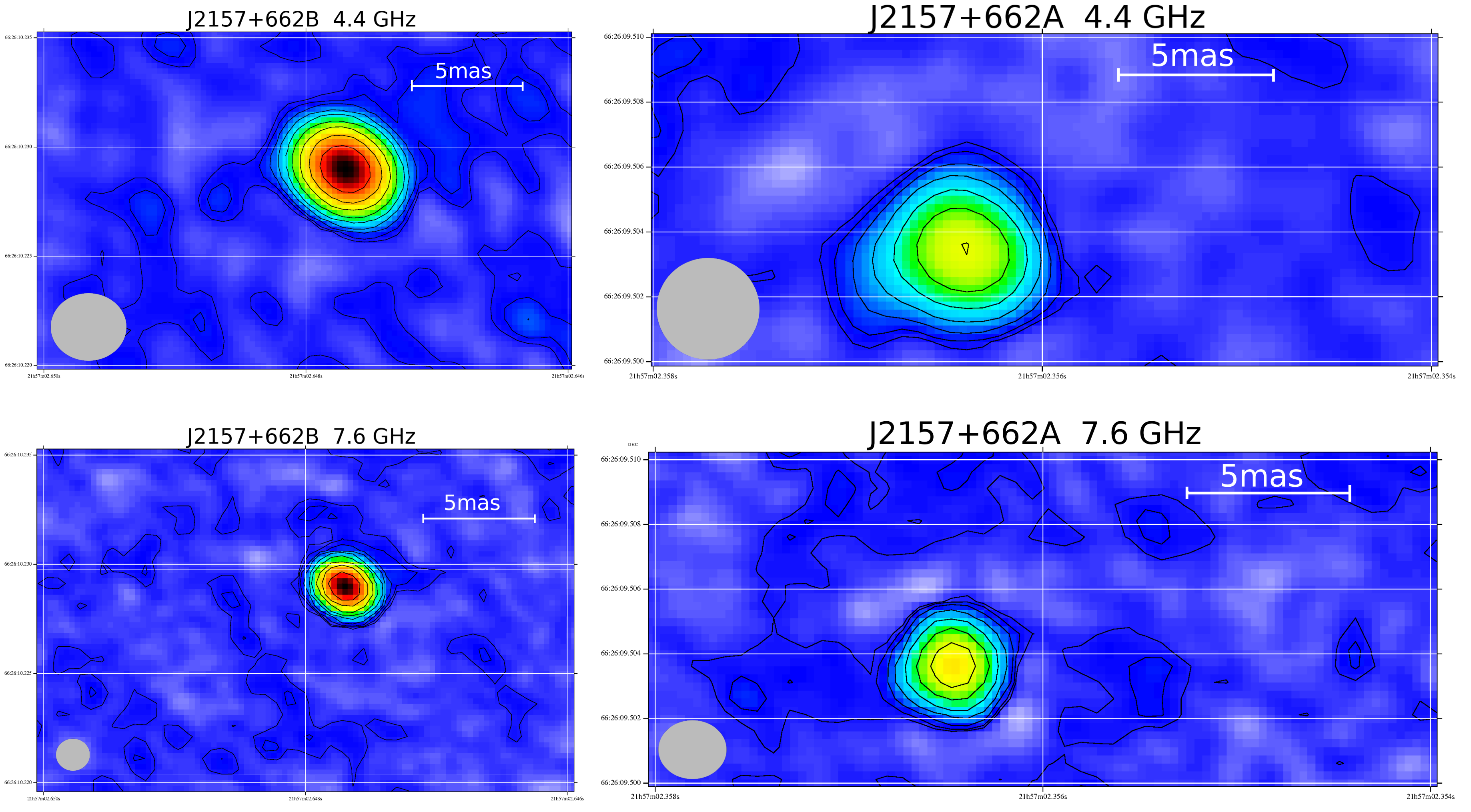

Adaptive optic image:

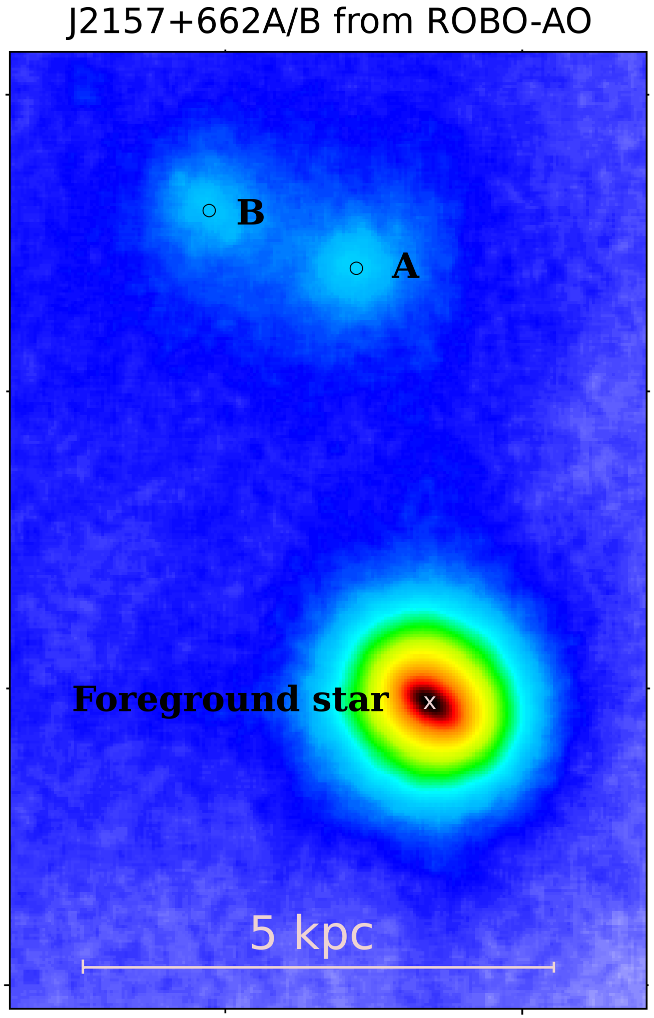

Possible interpretations:

1. Double AGNs at 2.1 kpc
2. Gravitational lens

Redshift 0.0584 is from absorption lines.
No emission line is detected.

Robo-AO is the first autonomous laser adaptive optics system currently in the commissioning phase at the the 2.1-m telescope at Kitt Peak National Observatory, AZ, USA.

Double galaxies:

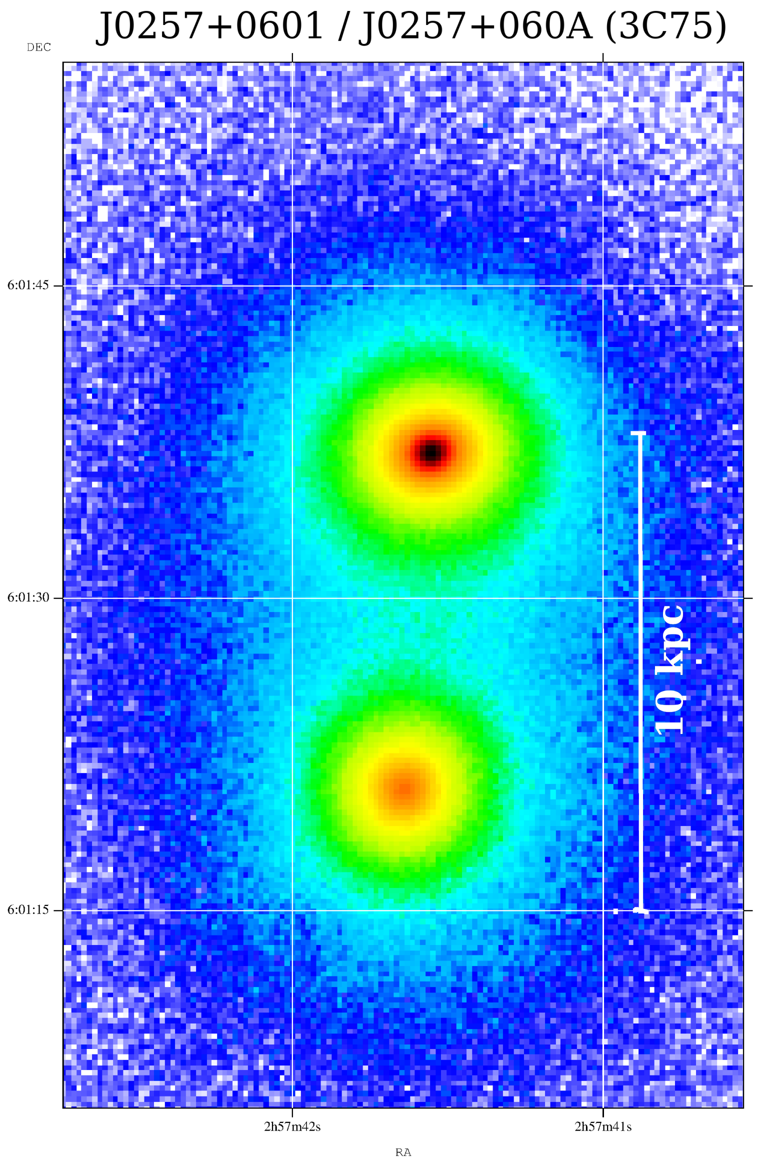

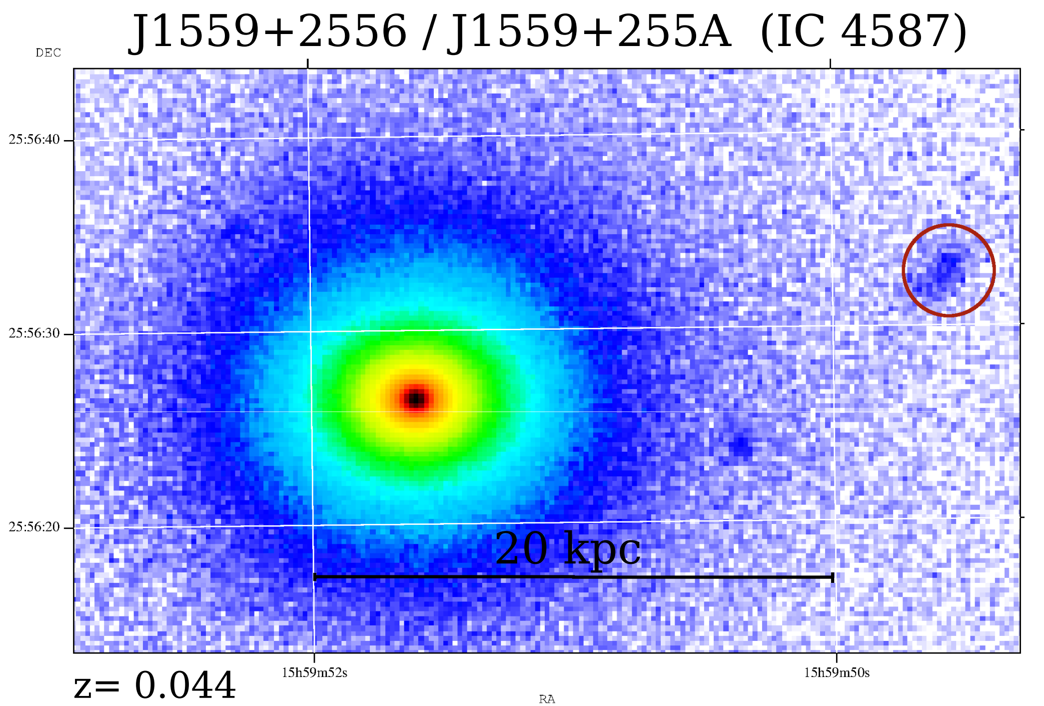

z= 0.044

Normalized variations of source density F(8.6GHz) > 160 mJy

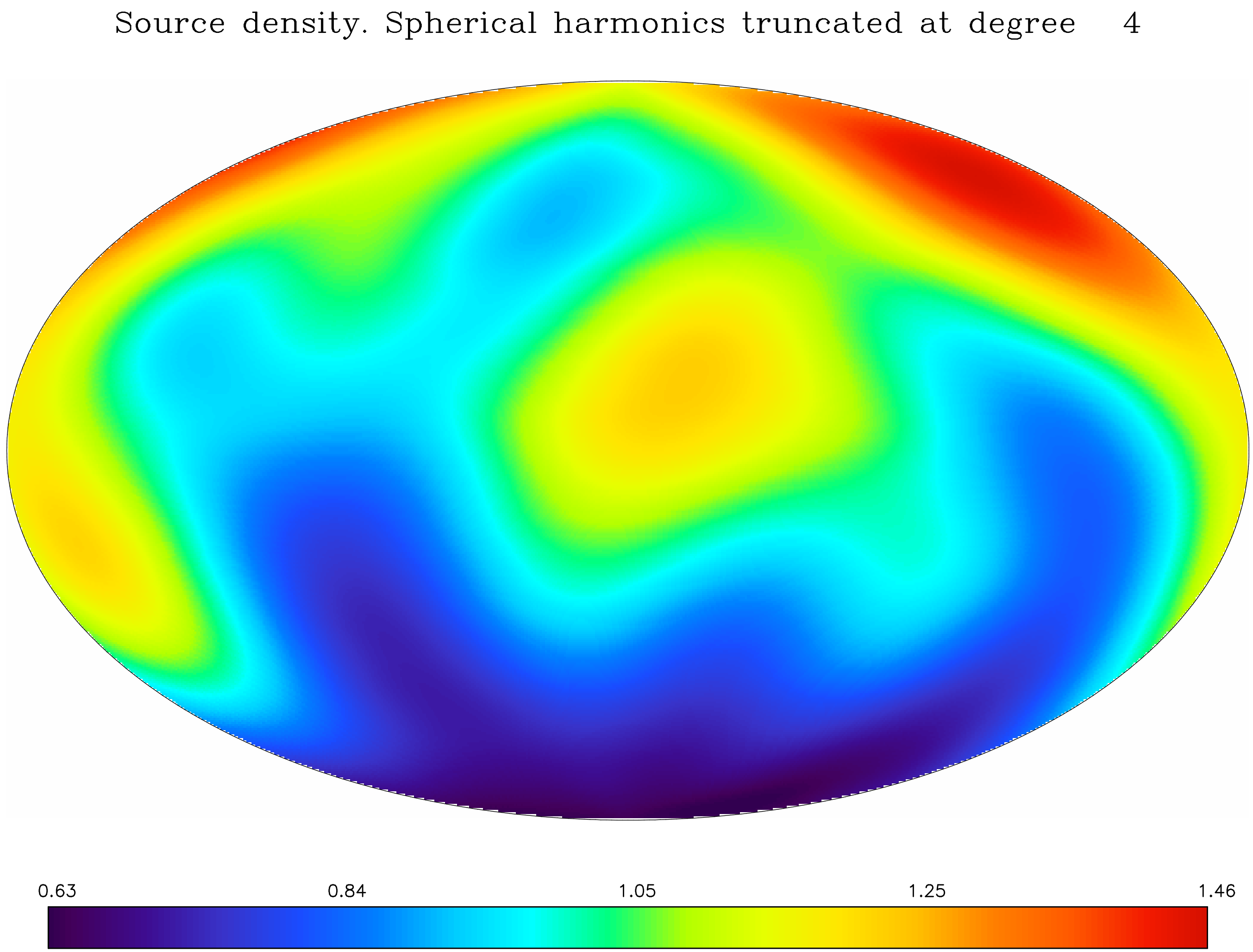

Normalized variations of source density F(8.6GHz) $>$ 160 mJy

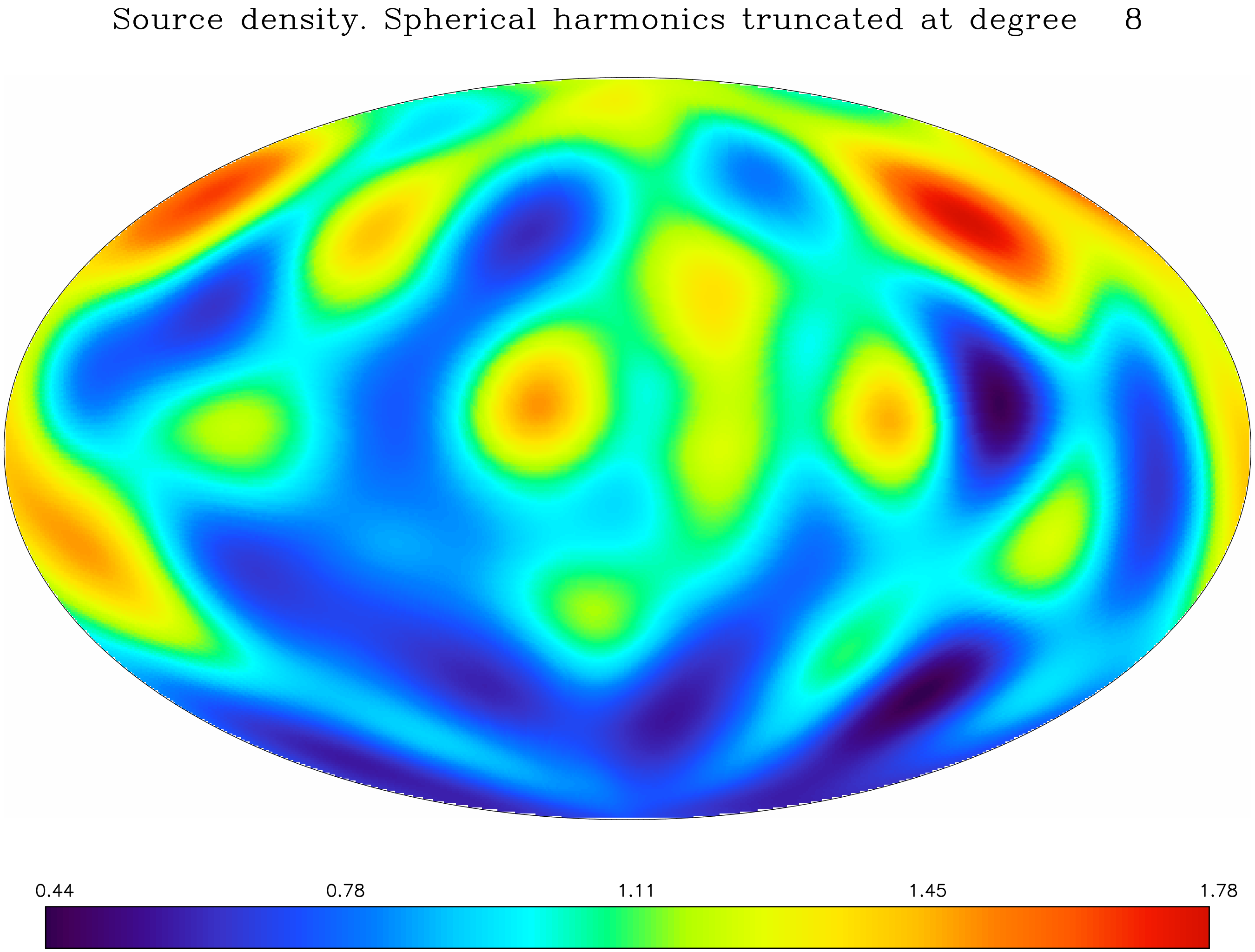

Normalized variations of source density F(8.6GHz) > 160 mJy

Source density. Spherical harmonics truncated at degree 16

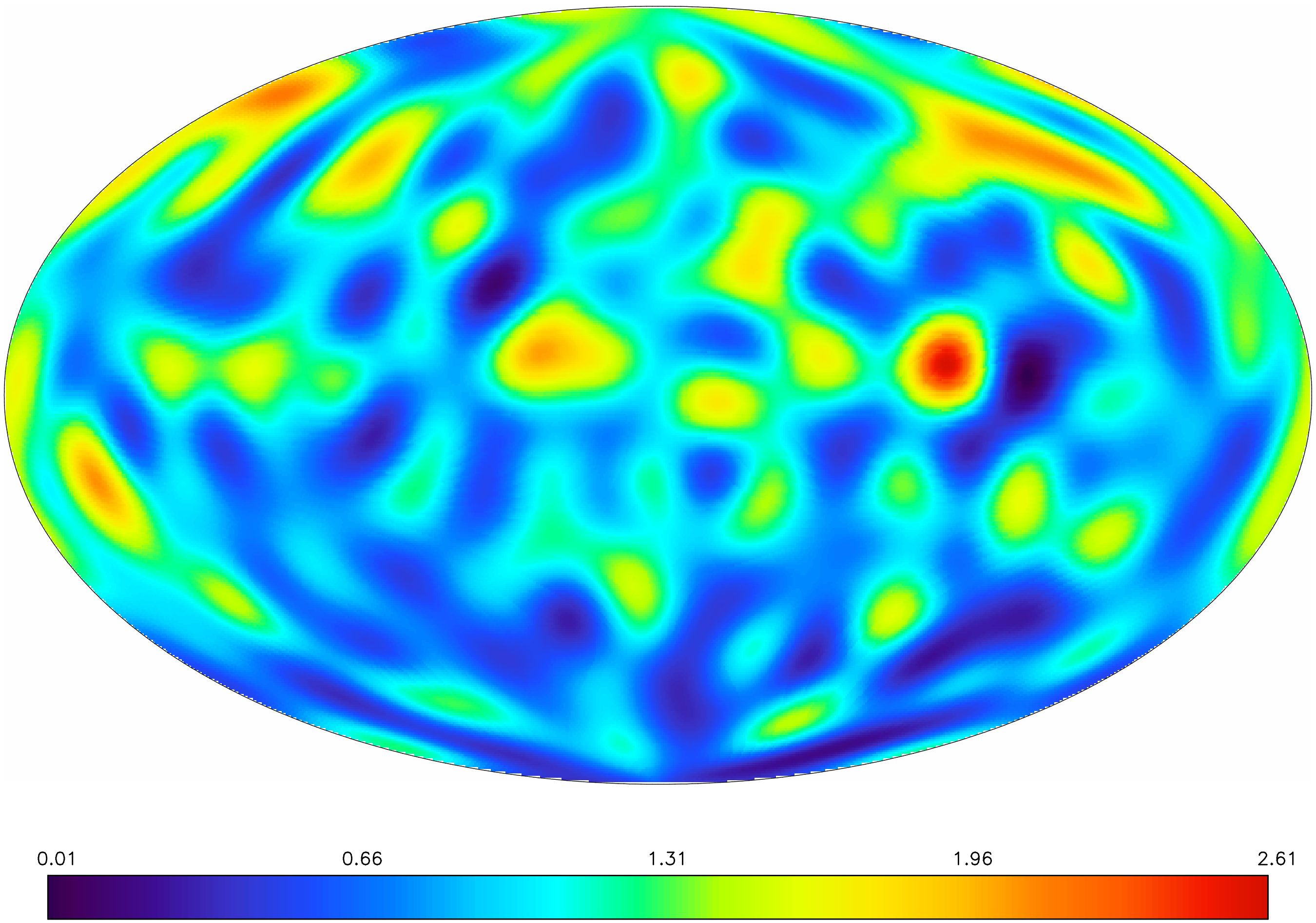

Multipoles of the source distribution F(8.6GHz) $>$ 160 mJy

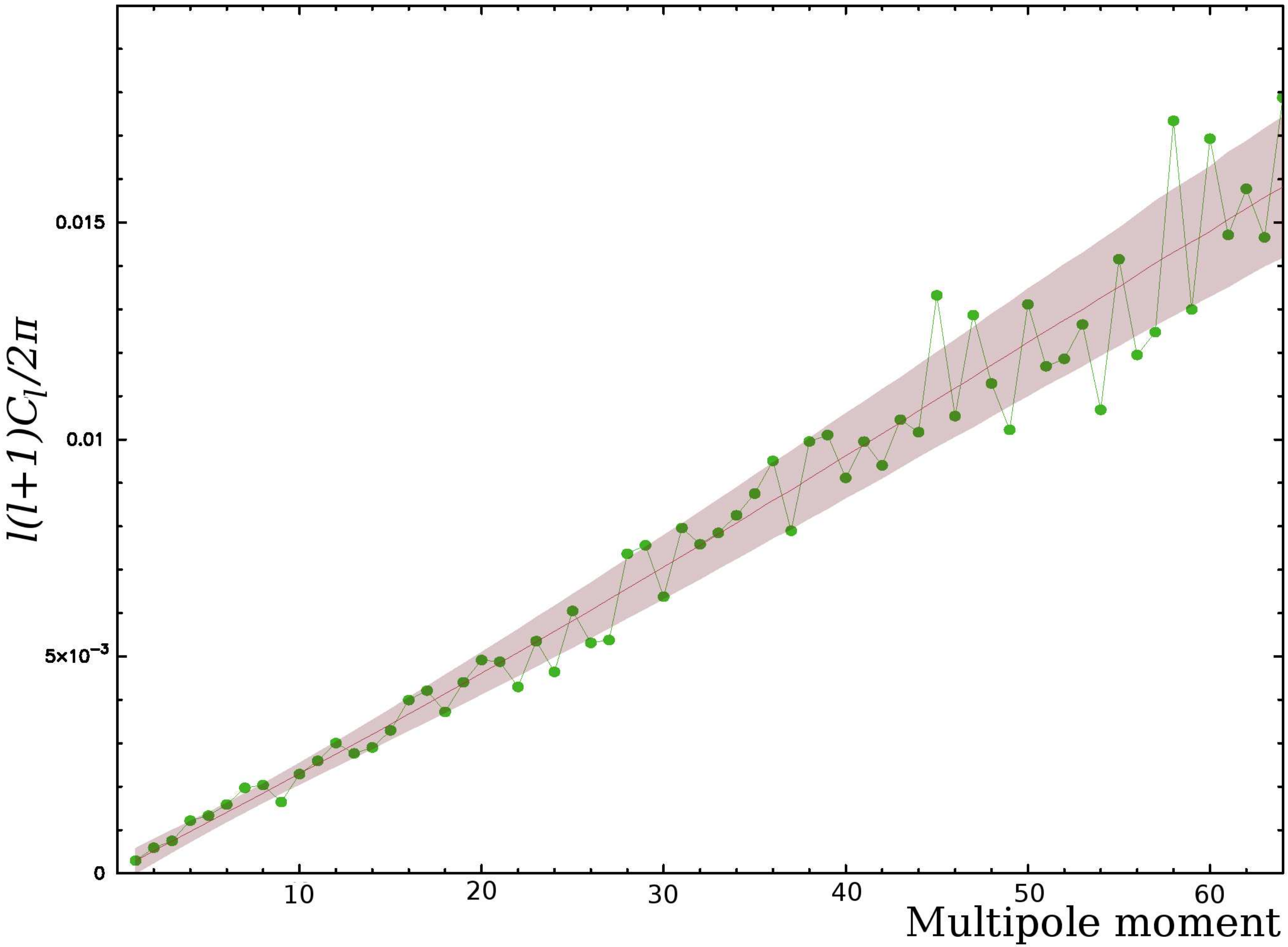

Red line shows results of simulation for the isotropic, uniform source distribution.

Core-shift and group delays

Let $\vec{s}_0$ be a reference position.

Core-shift causes source displacement $\vec{s}_0 + \kappa / f^r$.

$\tau_{\mathrm{geom},0}$ is geometric path delay to $\vec{s}_0$. Then $\tau_f = \tau_{\mathrm{geom},0} + \frac{\partial \tau}{\partial d} \frac{\kappa}{f^r}$, where d is unit direction of the core-shift.

Fringe phase are:

$$\phi = \phi_0 + 2\pi \, \tau_{\mathrm{geom},0}(f - f_0) + \dot{\tau}(t - t_0) + \frac{\partial \tau}{\partial d} \frac{\kappa}{f^{r-1}} - \frac{\partial \tau}{\partial d} f_0 \frac{\kappa}{f^r}$$

And when r = 1

$$\phi = \boldsymbol{\phi_0} + \mathbf{2}\pi \, \tau_{\mathrm{geom},0}(\mathbf{f} - \mathbf{f_0}) + \dot{\tau}(\mathbf{t} - \mathbf{t_0}) + \frac{\partial \tau}{\partial \mathbf{d}} \kappa - \frac{\partial \tau}{\partial \mathbf{d}} \mathbf{f_0} \, \kappa \, \frac{\mathbf{1}}{\mathbf{f}}$$

Porcas R. W., 2009, A&A, 505, L1

When r=1, core-shift is indistinguishable from the ionospheric contribution

Usually $r = 1$ (equipartition)

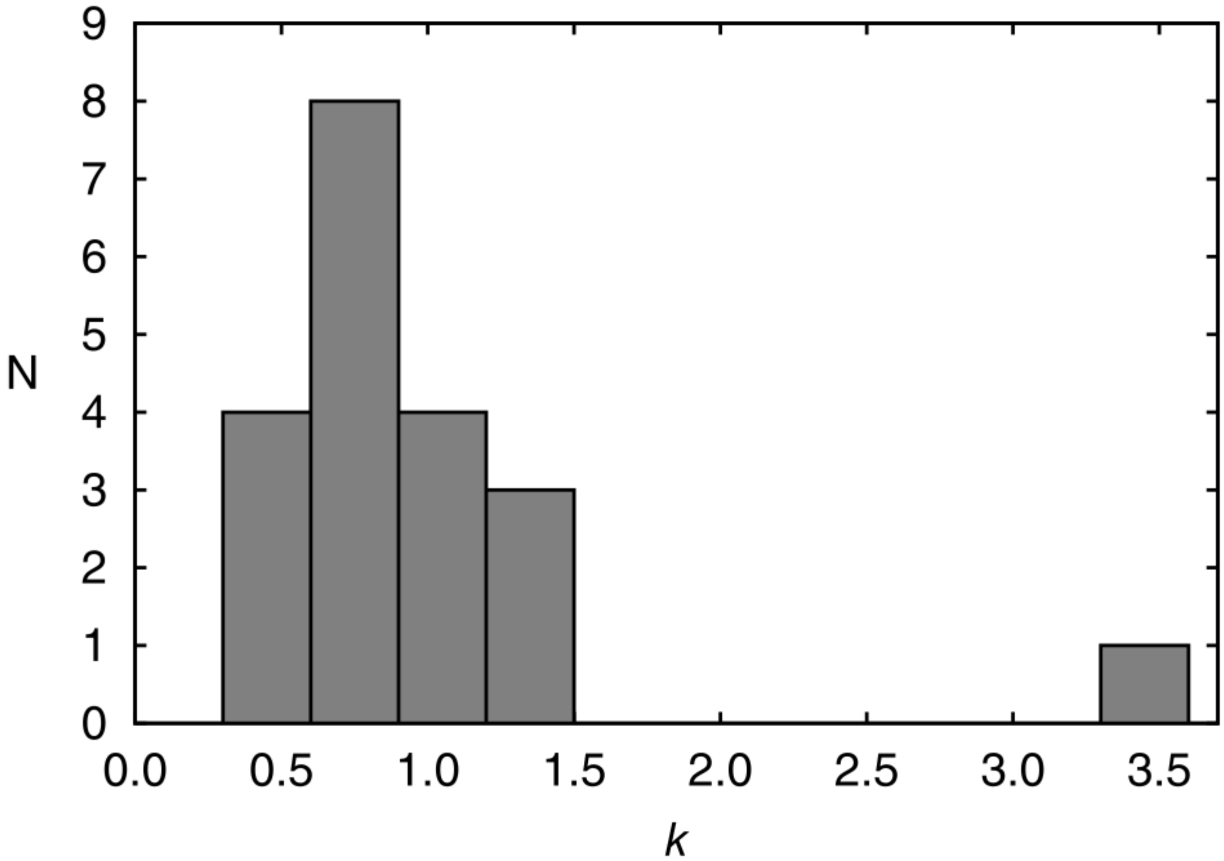

Fig. 5. Distribution of the k parameter in the core position as a function of frequency fit: $r_c(\nu) \propto \nu^{-1/k}$. The mean value is $k = 0.99 \pm 0.14$,

Sokolovsky et al, 2011

Core-shift is variable!

Core-shift variations correlate with flux density variations.

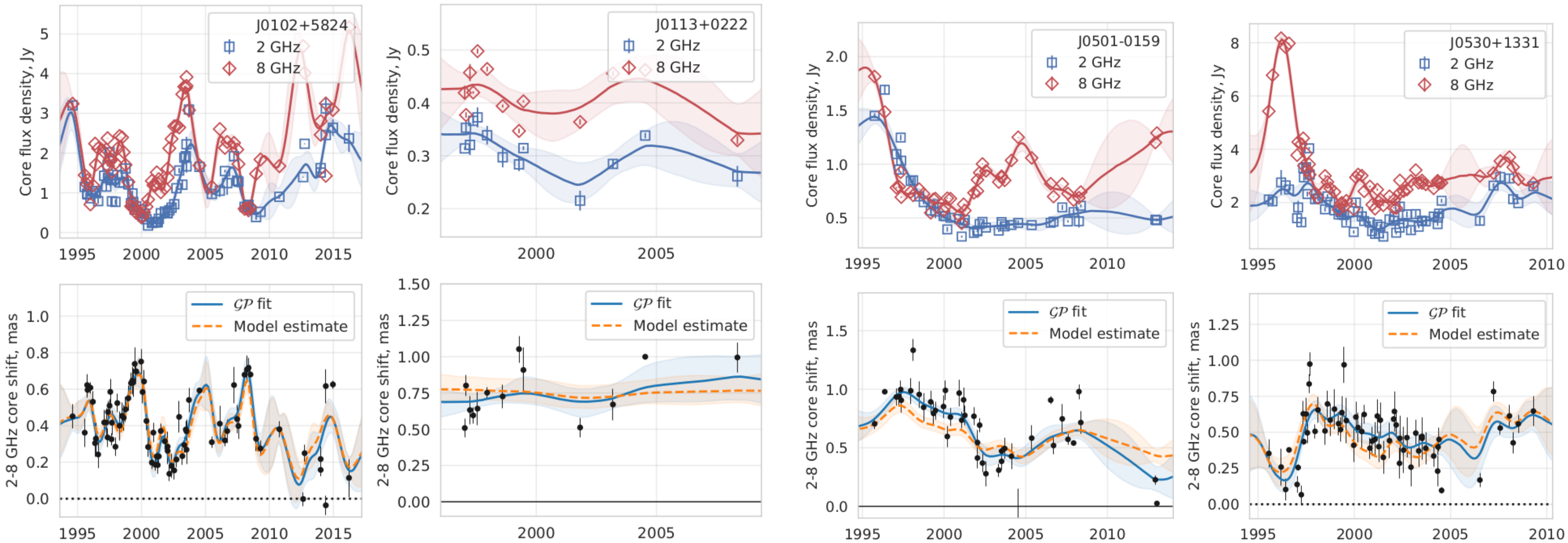

Plavin et al. 2019

Flares violate equipartition.

Therefore, core-shifts affects dual-band source position estimates during flares.

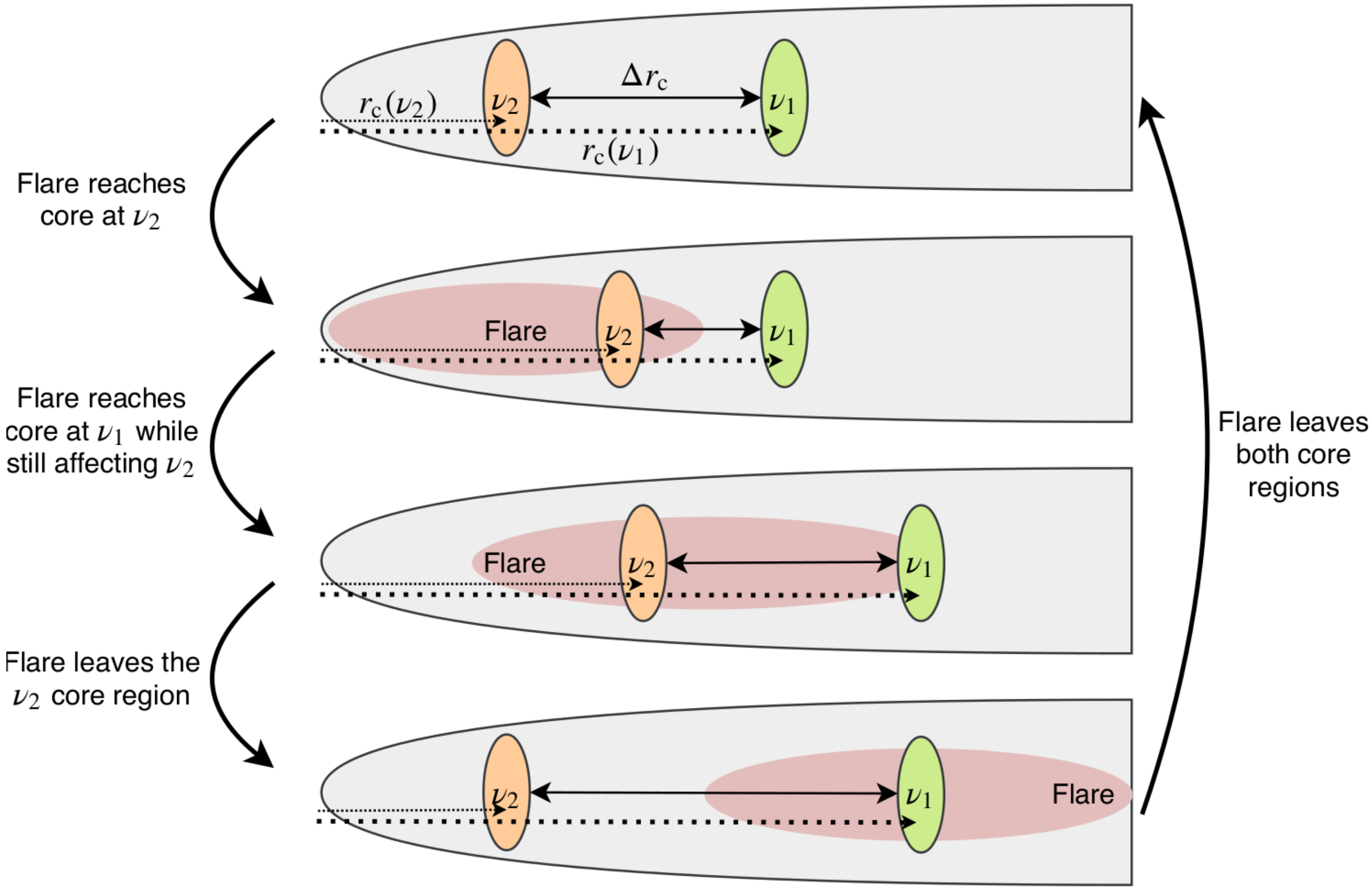

Plavin et al. 2019

Analyzing core-shift changes we can explore the optically-thick core

Can we see core-shift using absolute astrometry?

Direction of absolute position differences X band versus C band:

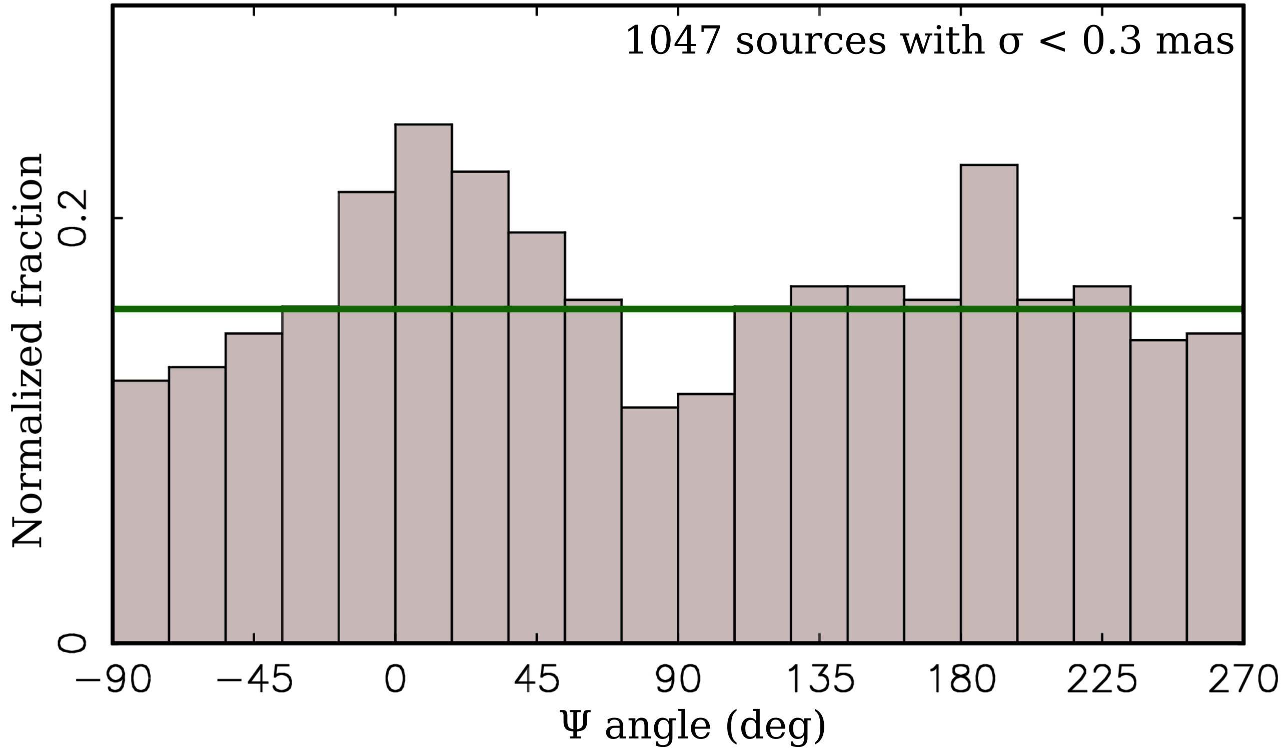

Core-shift is observable with absolute astrometry.

Part II. VLBI/Gaia comparison

Data

VLBI Radio Fundamental Catalogue (**16,466 sources**) on 2019.09.09 and *Gaia* DR2 ($1.69 \cdot 10^9$ objects)

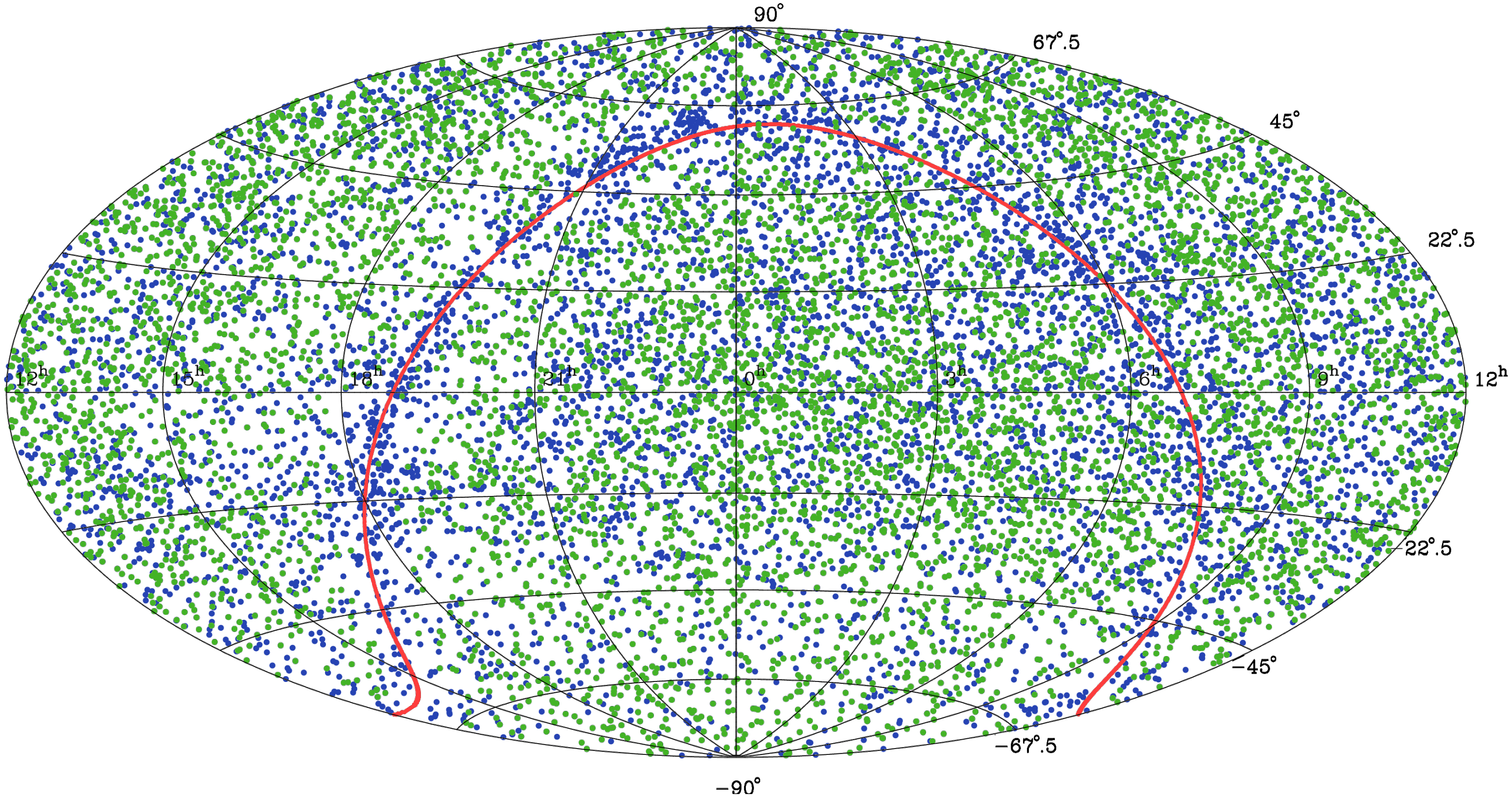

Green: 9,848 VLBI/*Gaia* matches $P < 0.0002$

Blue: VLBI sources without *Gaia* matches

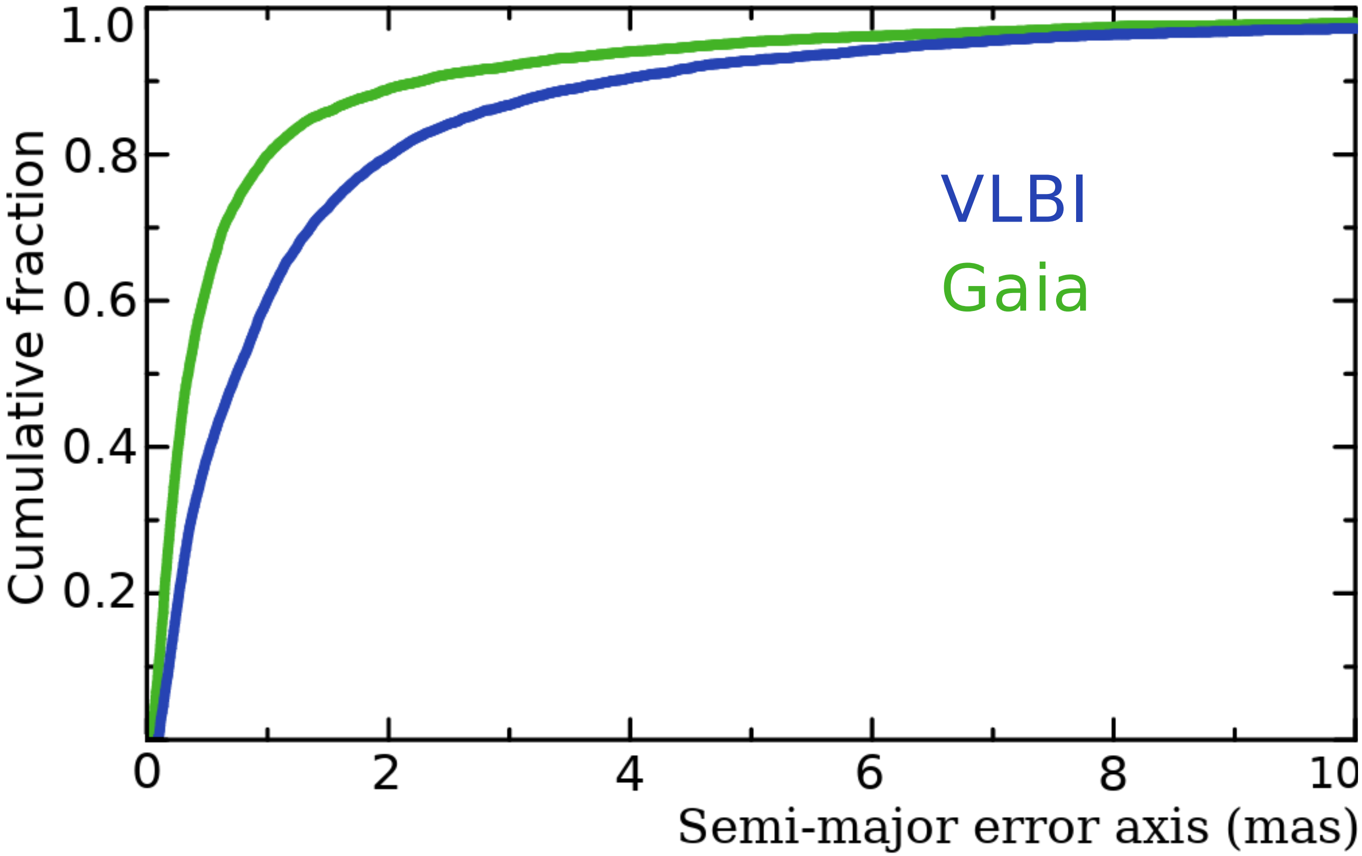

Median position error:

VLBI: 0.74 mas
Gaia: 0.34 mas

VLBI has lost its superiority to Gaia!

The distribution of normalized VLBI/Gaia arc-lengths over 9465 AGNs

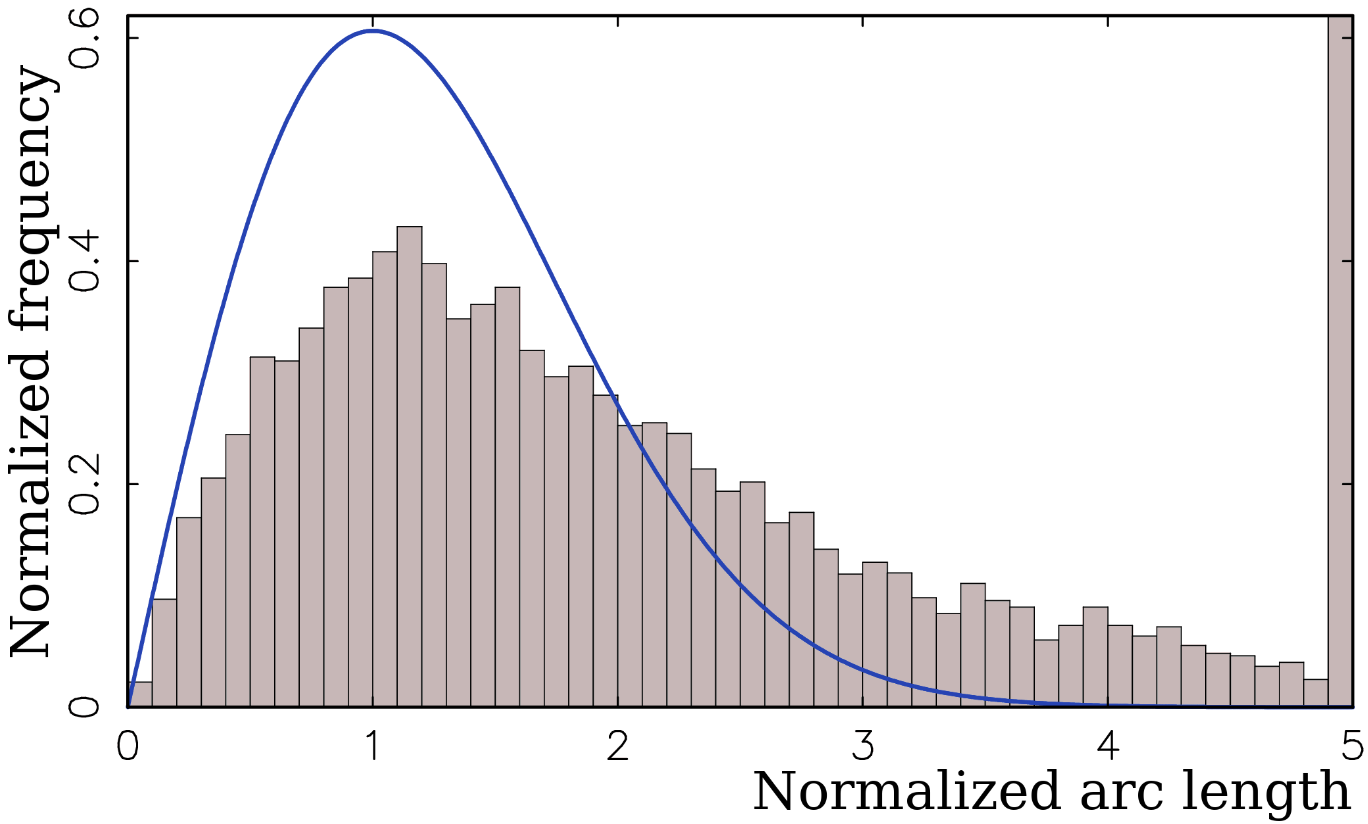

1/6 matched sources are outliers: $a/\sigma_a > 4$

What is their nature?

Distribution of VLBI/Gaia position offset angles

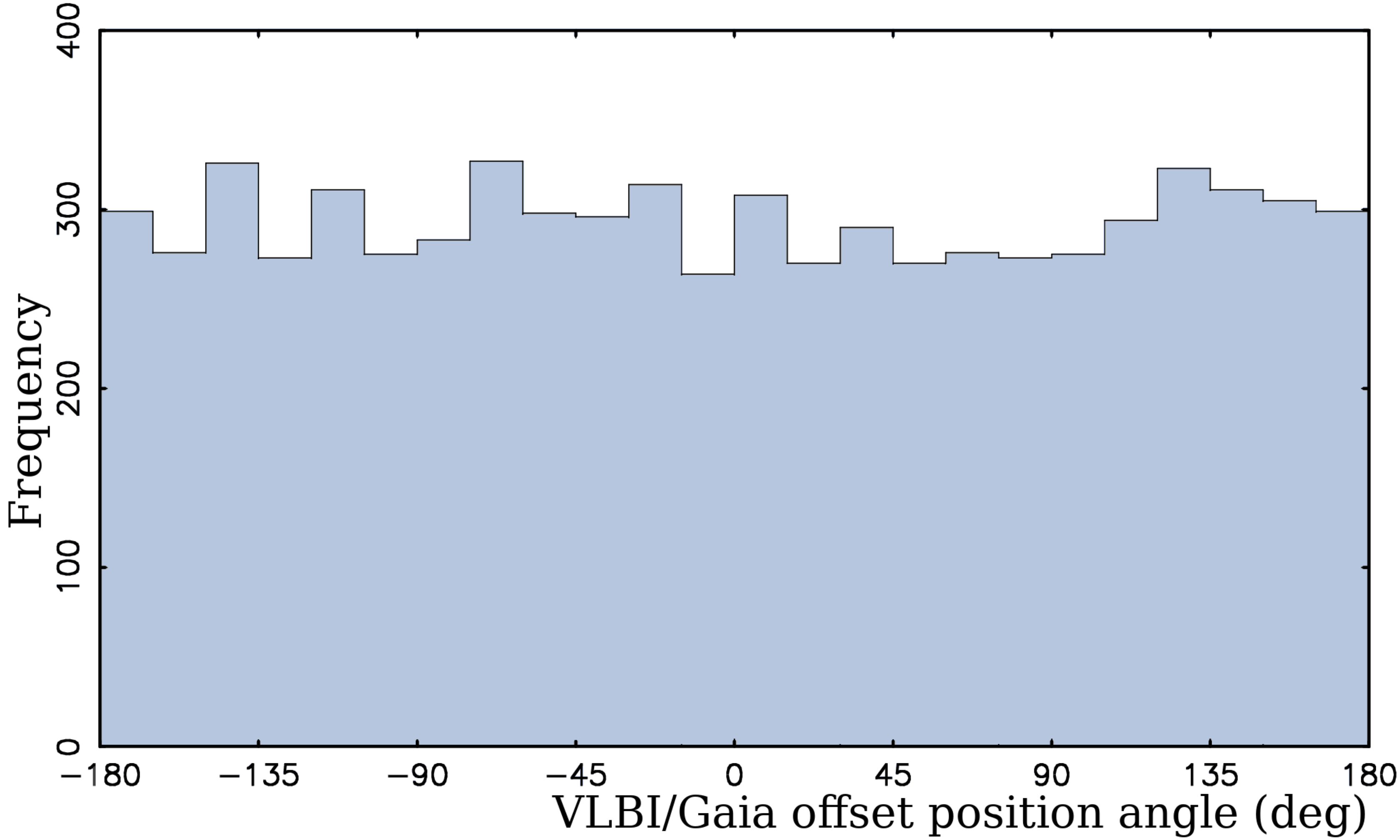

Main finding: no preference at $0°, 180°$ (VLBI declination errors)
No deviation from the isotropy.

Distribution of AGN jet directions in the VLBI/Gaia sample

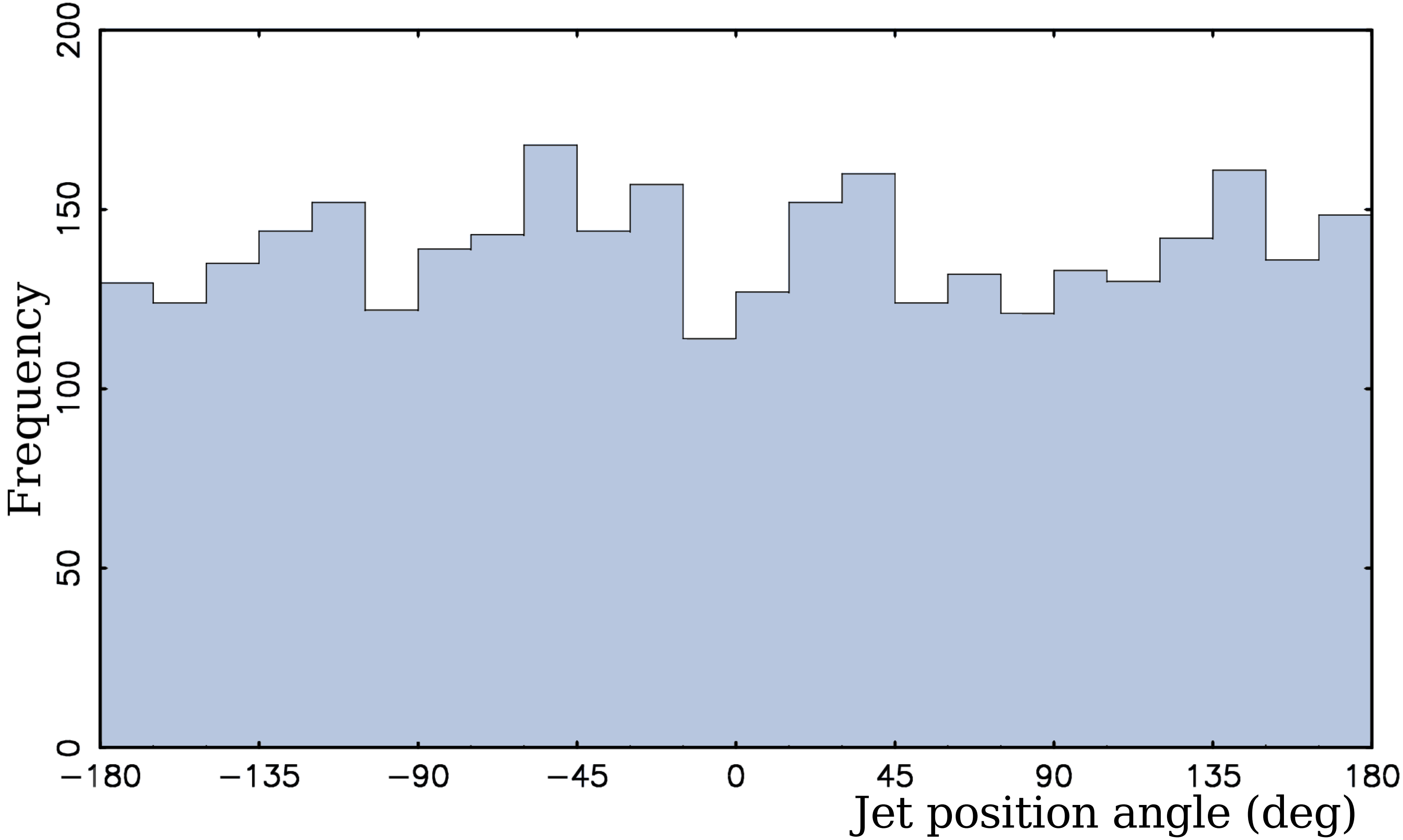

No deviation from the isotropy

Distribution of VLBI/Gaia position offset angles with respect to jet direction

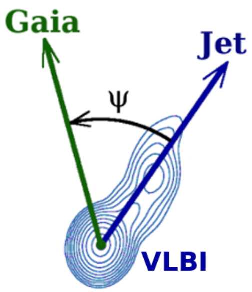

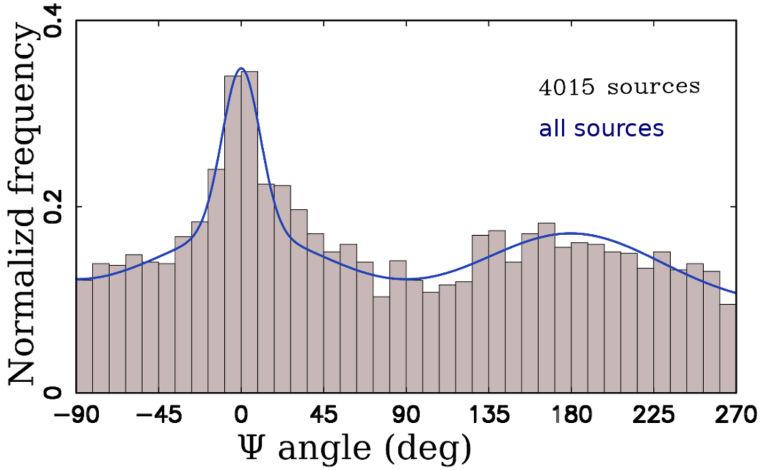

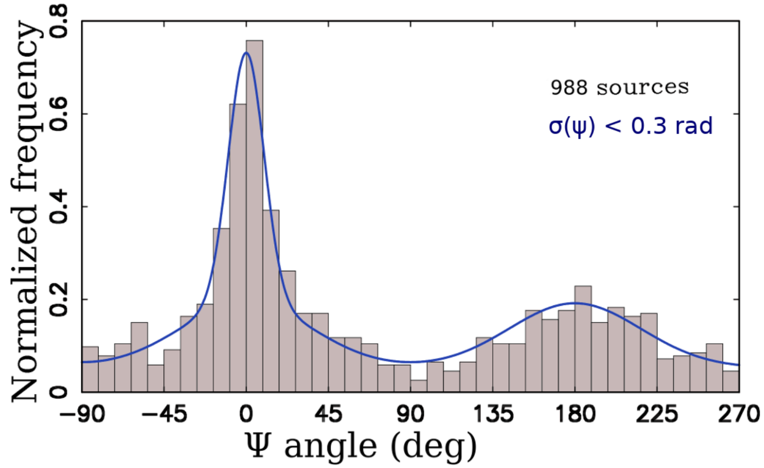

Centroid of a core-jet morphology

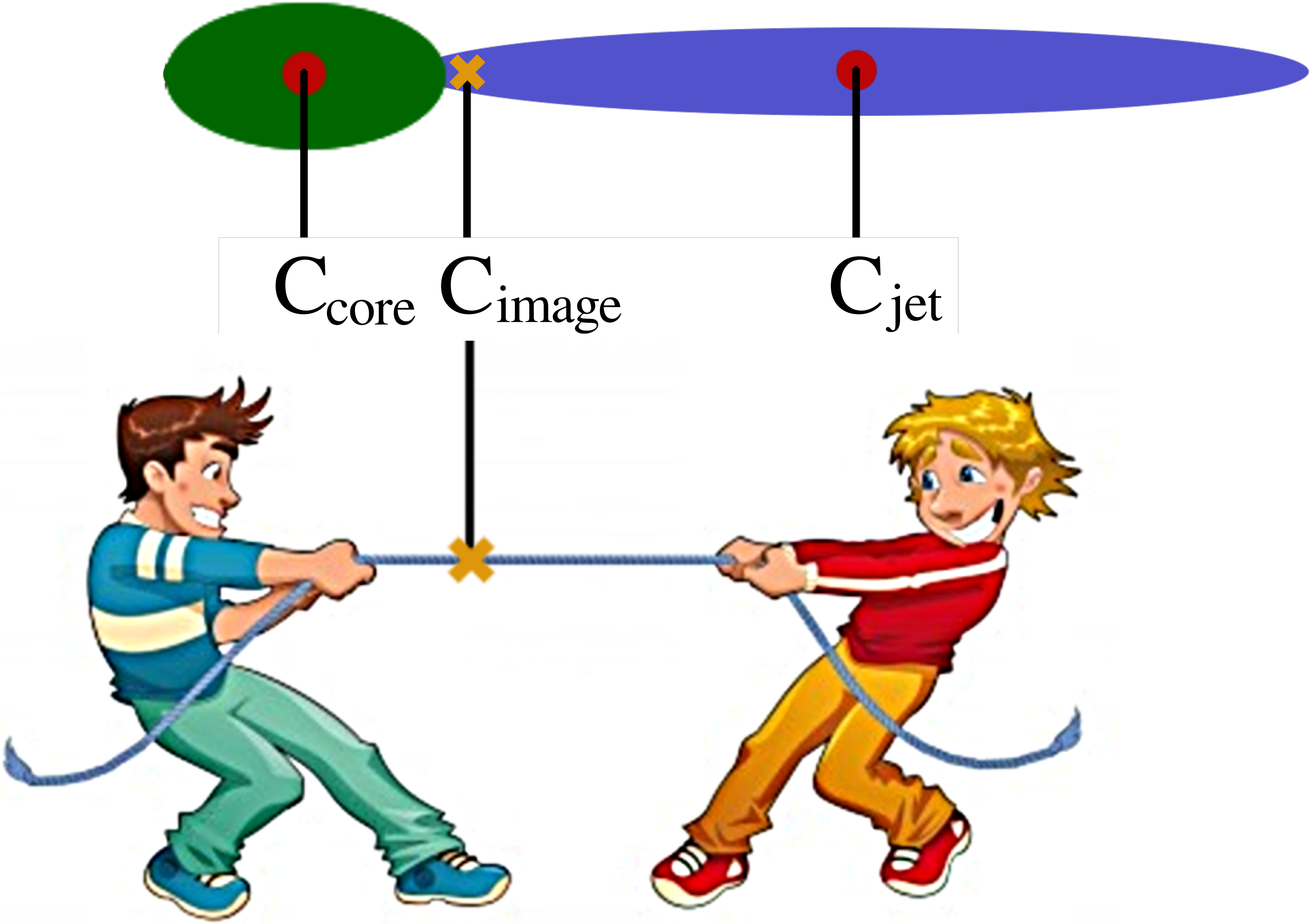

Contribution of optical structure

There are over 20 known optical jets with sizes 0.5–$20''$

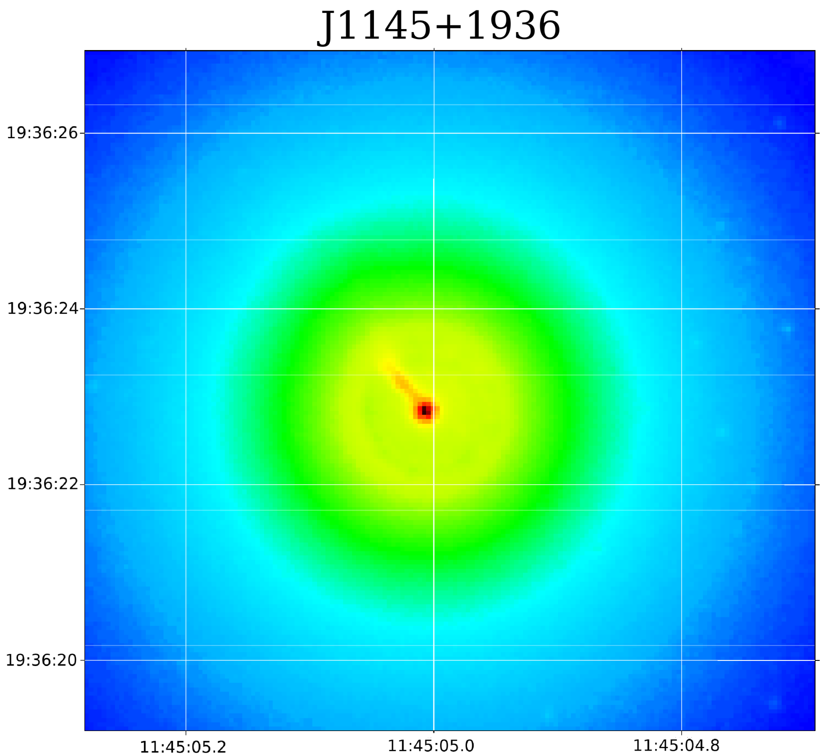

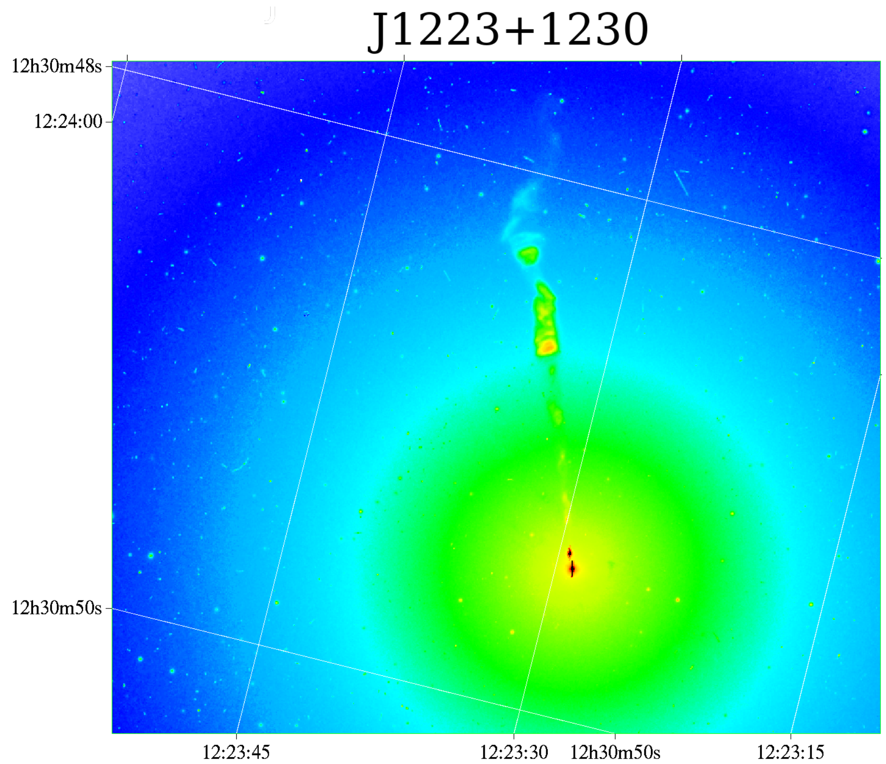

At z=0.07, visible optical jet of J1145+1936 would shift centroid at 5 mas

At z=0.3, visible optical jet of J1223+1230 would shift centroid at 1.2 mas

Conclusion: known optical jets at farther distance can cause centroid shifts at 1–2 mas level

Direction of the centroid change after a flare

- 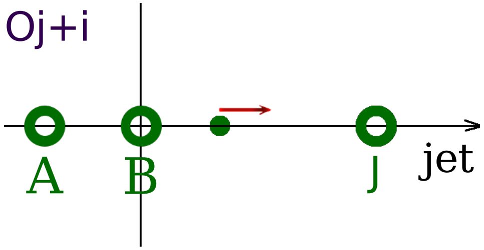

Flare happened at the jet

- 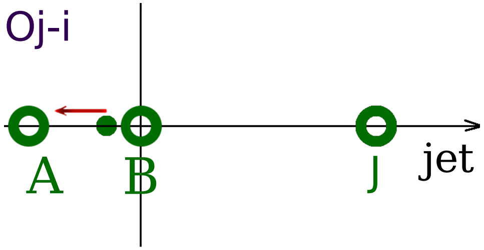

Flare happened at the accretion disk

- 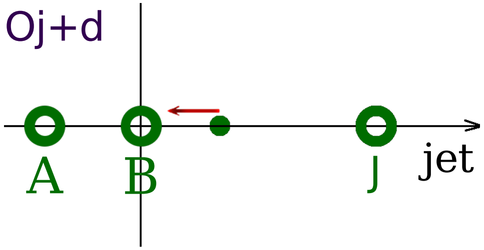

Flare happened at the core or the accretion disk

- 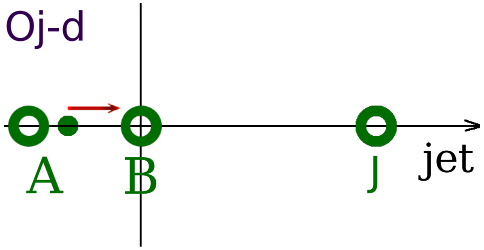

Flare happened at the core or the jet

Consequences of the optical jet interpretation for VLBI/Gaia offsets

Astrometry:

1. **VLBI** and **Gaia** positions cannot be reconciled

2. **Gaia** position accuracy cannot be used for radio applications

3. We predict a jitter in **Gaia** positions

Consequences of the optical jet interpretation for VLBI/Gaia offsets

Astrophysics:

1. Joint analysis of **VLBI**/**Gaia** time series and **optical light curves** will allow
   1.1. pin-point the region where flares occur
   1.2. estimate effective size of optic jet and its relative flux
2. **VLBI**/**Gaia** offsets will correlate with color
3. AGN optical image in orthogonal polarizations wrt jet direction will have an offset
4. AGNs with large **VLBI**/**Gaia** will have higher fractional polarization in optical range

Directions of Gaia and VLBI proper motions

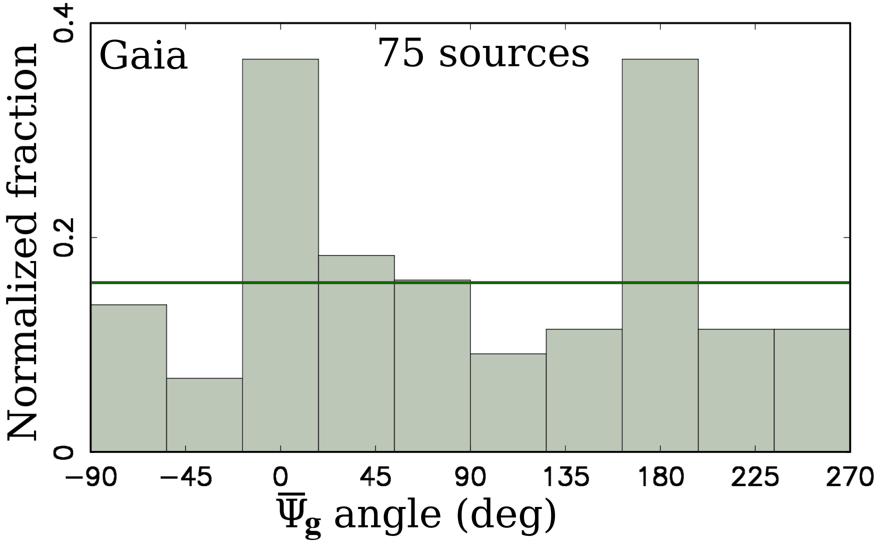

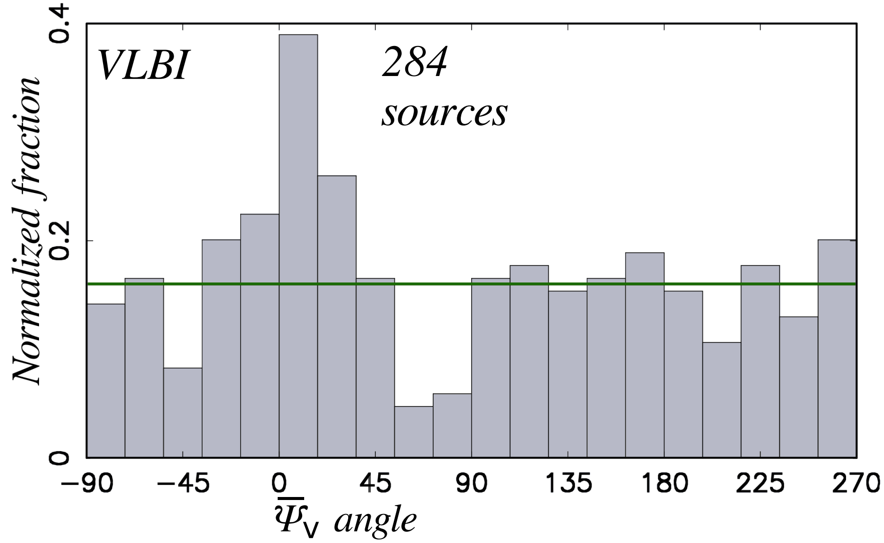

Only proper motions greater 4σ are accounted

Median proper motions:

Gaia: 1.2 mas/yr

VLBI: 0.02 mas/yr

Dependence of Gaia proper motion direction on $\chi^2/$ndf

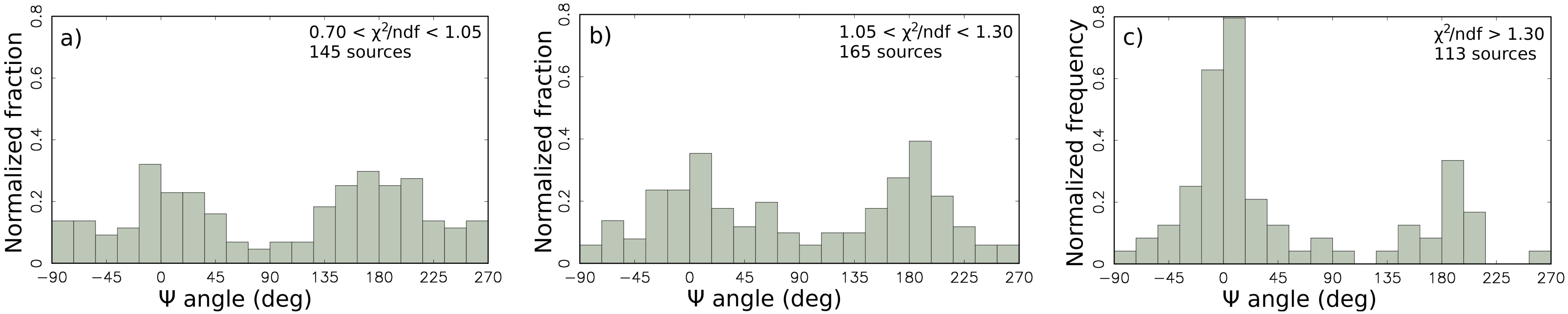

Only sources with $\sigma_{\bar{\psi}} < 0.3$ rad and arc-lengths < 2.5 mas are accounted

$$\chi^2/ndf \textit{ is a measure of non-linearity of AGN motion}$$

Stronger non-linearity is associated with proper motion along the jet direction.

2D Ψ-angle/VG distance distribution

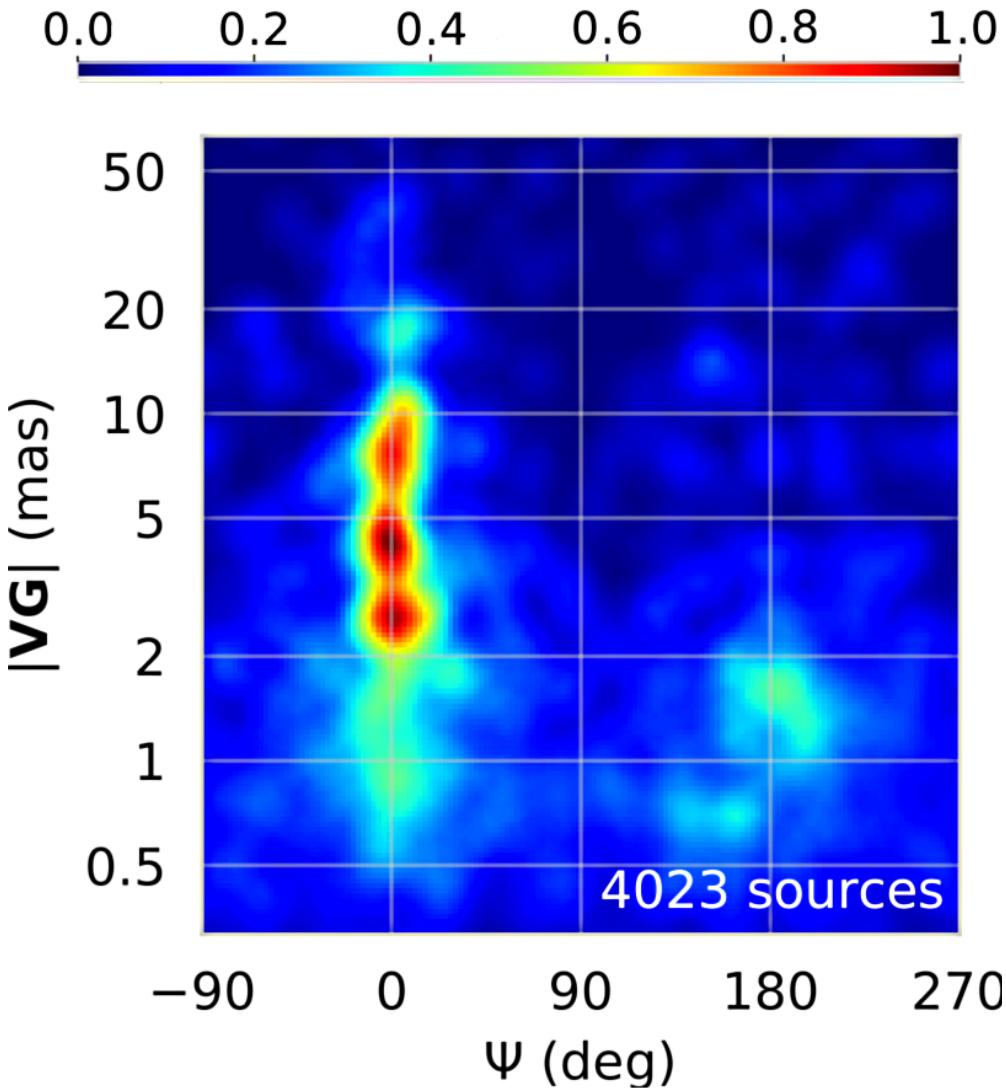

2D Ψ-angle/VG distance distribution

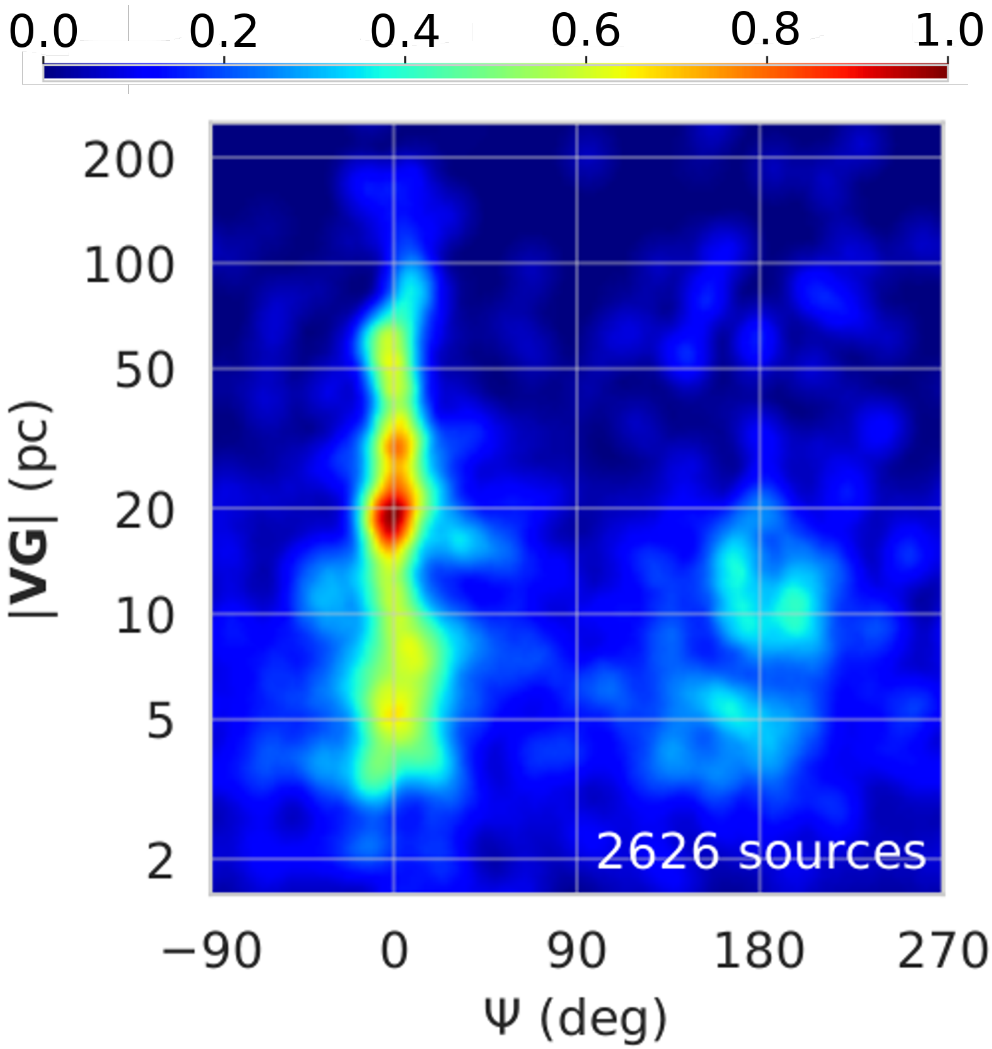

2D Ψ-angle/redshift and Ψ-angle/color distribution

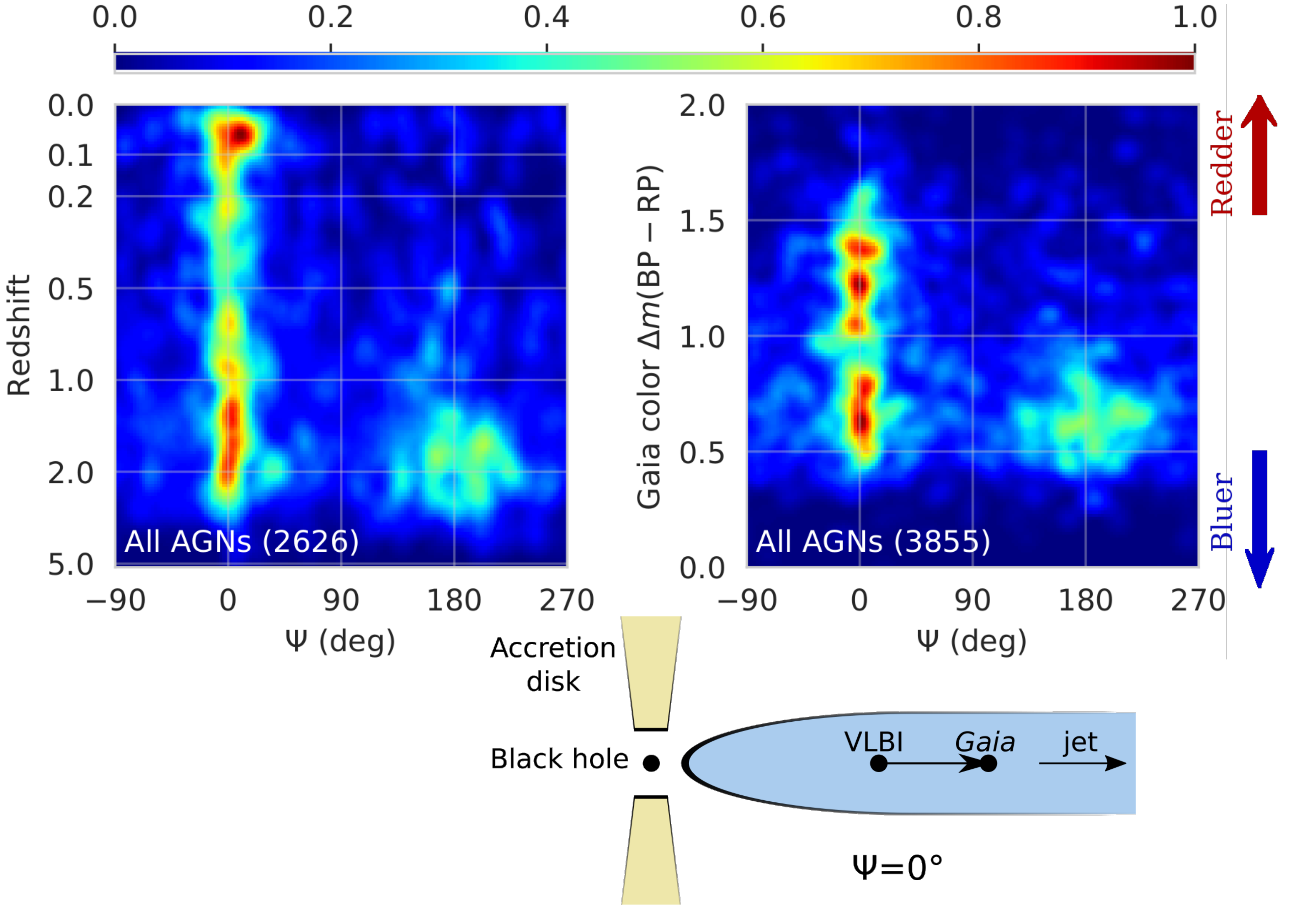

2D Ψ-angle/color distribution for different AGN types

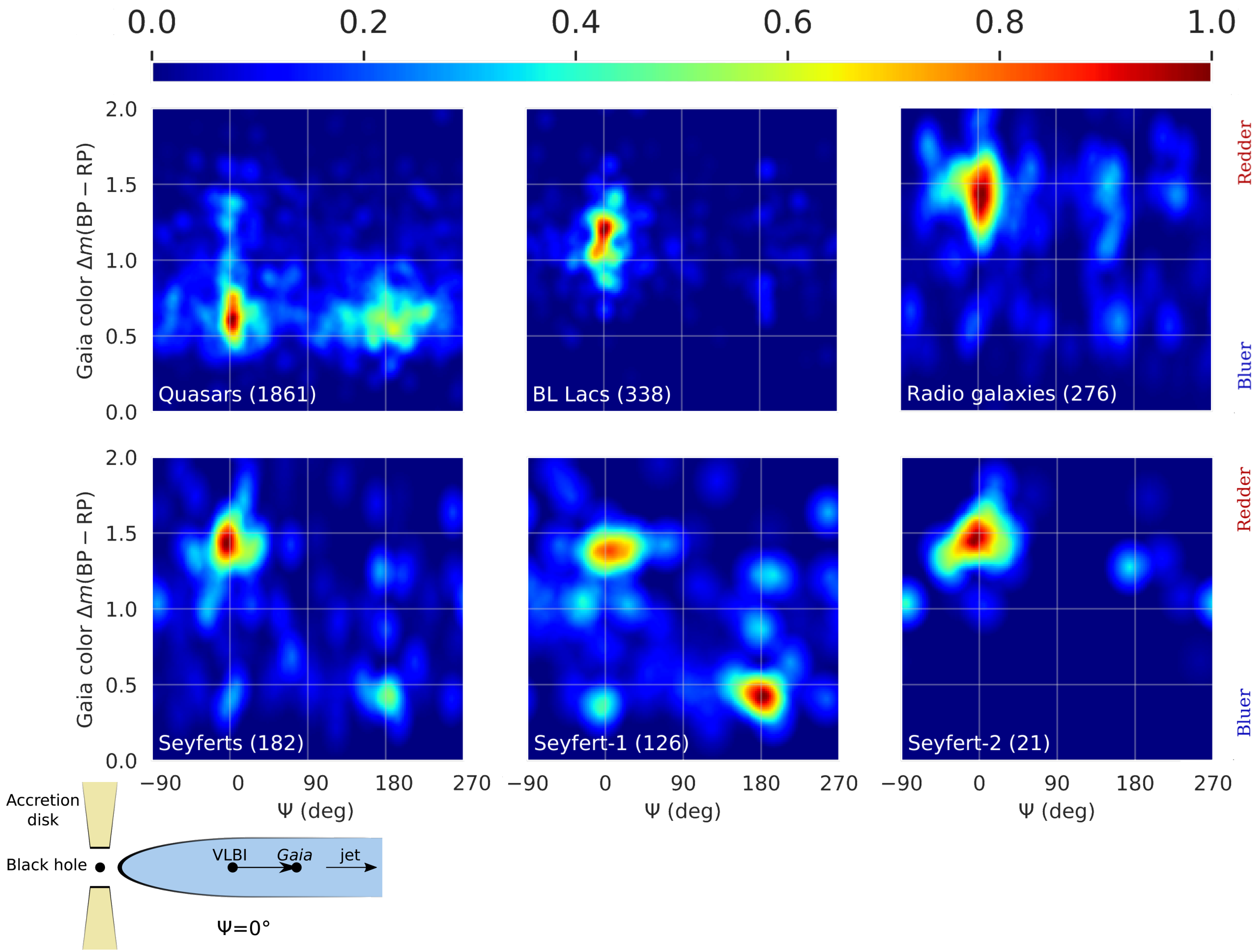

Summary

VLBI surveys yielded positions of 16,466 objects and images of 14,076 sources.

Using the VLBI catalogue, we can

- study Earth rotation, runs space geodesy and space navigation programs
- study the anisotropy of AGN distribution
- study the population of radio-load AGNs
- associate γ-ray sources
- explore the optically thick AGN core
- study optical jets at mas resolution
- determine the origin of flares
- distinguish sources with accretion disk and synchrotron dominated optical emission